



Published in final edited form as:

Biomater Adv. 2022 March ; 134: 112576. doi:10.1016/j.msec.2021.112576.

3D bioprinting and photocrosslinking: emerging strategies & future perspectives

Allen Zennifer^{a,1}, Sweda Manivannan^{a,1}, Swaminathan Sethuraman^a, Sangamesh G. Kumbhar^b, Dhakshinamoorthy Sundaramurthi^{a,*}

^aTissue Engineering & Additive Manufacturing (TEAM) Lab, Centre for Nanotechnology & Advanced Biomaterials (CeNTAB), ABCDE Innovation Centre, School of Chemical & Biotechnology, SASTRA Deemed University, Tamil Nadu 613 401, India

^bDepartment of Orthopedic Surgery, University of Connecticut Health Center, 263 Farmington Avenue, Farmington CT-06030-4037, USA

Abstract

3D bioprinting has enabled the creation of biomimetic tissue constructs for regenerative medicine and *in vitro* model systems. Large-scale production of 3D structures at the micron-scale resolution is achieved through bioprinting using custom bioinks. Stability and 3D construct compliance play an important role in offering cells with biomechanical cues that regulate their behavior and enable *in vivo* implantation. Various crosslinking strategies are developed to stabilize the 3D printed structures and new methodologies are constantly being evaluated to overcome the limitations of the existing methods. Photo-crosslinking has emerged as a simple and elegant technique that offers precise control over the spatiotemporal gelation of bioinks during bioprinting. This article summarizes the use of photo-crosslinking agents and methodology towards optimizing 3D constructs for specific biomedical applications. The article also takes into account various bioinks and photo-crosslinkers in creating stable 3D printed structures that offer bioactivity with desirable physicochemical properties. The current challenges of 3D bioprinting and new directions that can advance the field in its wide applicability to create 3D tissue models to study diseases and organ transplantation are also summarized.

Keywords

Photo-crosslinking; Hydrogels; Additive manufacturing; 3D bioprinting; Bioinks; Tissue engineering

*Corresponding author at: Tissue Engineering & Additive Manufacturing (TEAM) Lab, Centre for Nanotechnology & Advanced Biomaterials (CeNTAB), ABCDE Innovation Centre, Anusandhan Kendra—1, School of Chemical & Biotechnology, SASTRA Deemed University, Tirumalaisamudram, Thanjavur 613 401, Tamil Nadu, India., dhakshinamoorthy@scbt.sastra.edu (D. Sundaramurthi).

¹These authors have contributed equally to this work.

Declaration of competing interest

Authors declare that they have no conflict of interest.

1. Introduction

Tissue engineering is a multidisciplinary field that aims to fabricate bio-mimetic three-dimensional scaffolds using the combination of cells, biomaterials, and growth factors. Generally, the applications of tissue engineering aim to repair or regenerate damaged tissues or organs such as skin, bones, nerves, to name a few using functional three-dimensional (3D) scaffolds. Various conventional scaffold fabrication techniques such as solvent casting, particle leaching, gas foaming, freeze-drying, thermal-induced phase separation, and electrospinning have been adopted successfully to develop 3D scaffolds [1]. Some of the scaffold fabrication procedures may also involve gene or immunomodulatory techniques to recapitulate the functionalities of native tissues. However, the use of these techniques was restricted due to consequent disadvantages such as inhomogeneity in pore geometry, nutrient and gaseous diffusion limitations in thicker scaffolds, limited blood vessel formation, poor resolution in scaffold architecture, and a time-consuming process. [2]. Therefore, modern scaffold fabrication techniques such as 3D molding, fused deposition modeling (FDM), selective laser sintering (SLS), and 3D printing have been widely used nowadays. These techniques enable the fabrication of constructs with controllable interconnected porous nature, 3D precision, better resolution, faster process with less human errors, and better vasculature, which enhances mass transfer in thicker scaffolds. Furthermore, there are also reports suggesting the implementation of these 3D bioprinted constructs as *in vitro* models for drug screening and pharmacokinetics applications [3]. Among these modern methods, 3D bioprinting is an additive manufacturing technique utilized to develop suitable biomimetic structures with complex anatomical patterns using a bioink, which comprises cells and polymers [4]. Typically, the required structures are modeled, digitized, and fed into the bioprinter using 3D modeling software such as computer-aided design (CAD), computer-aided manufacturing (CAM). Largely, these input digital files are derived from target tissues or organs of patients using imaging modalities such as nano/micro-computed tomography (CT), magnetic resonance imaging (MRI). 3D bioprinting is a fabrication process that involves the printing of scaffolds in a “layer-by-layer” fashion, such that one layer is printed and gets solidified before the next layer is deposited. This will result in a temporary framework, which acts as an adhesive layer for cells to perform cell modulatory activities and to deliver growth factors to the cells in a regulated manner [5]. Thus, the bioinks should possess remarkable properties such as good cytocompatibility, native biological cues with desired degradation rate, suitable rheological & mechanical properties, instant crosslinking ability, provide shape fidelity and offer ease of processability [6].

Natural or synthetic polymers such as collagen, gelatin, silk fibroin, alginate, poly(ethylene glycol) (PEG), and poly(caprolactone) (PCL) are widely used as bioink materials. During the bioprinting process, these bioinks form hydrogels *via* various crosslinking strategies and become stable 3D structures [7]. Crosslinking processes are broadly classified into physical and chemical methods based on the mechanism of action. Among these methods, chemical methods are widely used because of their wide range of tunability and stability under physiological conditions [8]. On the contrary, physical crosslinking occurring *via* secondary forces such as hydrophobic interactions, hydrogen bonding or van der Waals forces would result in constructs with weak mechanical stability and hence may not be

suitable for the long term *in vitro* culture studies [9]. Importantly, the choice of crosslinking method depends on the biopolymer backbone, functional side groups & their crosslinking mechanism, and other required supplementary chemicals. Considerations of these multiple factors for choosing an efficient crosslinking strategy is very essential as it has a significant impact on the cytocompatibility, mechanical, physiochemical, and cellular behavior of the resultant construct [10].

Among different chemical crosslinking methods, photocrosslinking is one of the most commonly employed approaches in 3D bioprinting due to its higher crosslinking efficiency and spatiotemporal controllability in developing sustainable tissue constructs [11]. These superior features of photocrosslinking have directed to wide-ranging applications of tunable hydrogels for various applications. This method utilizes photoinitiators and photo-reactive polymers to enable photoinduced covalent bond formation by simply adjusting certain working parameters such as light source, the intensity of light, exposure time, and area of illumination [11]. For instance, natural biopolymer gelatin is chemically modified into photoreactive gelatin methacrylate (GelMA) using methacrylic anhydride [12]. GelMA undergoes free-radical crosslinking in presence of photoinitiators (Irgacure 2959) under UV light of the wavelength of 360–380 nm and forms chemically stable 3D photocrosslinked gelatin (Fig. 1). This type of photo-induced polymerization allows prepolymer solutions to be tuned into stable hydrogels with a desirable degradation profile and mechanical behavior.

In general, photocrosslinking of biopolymers can be performed at various stages during the bioprinting process such as pre-crosslinking, postcrosslinking, and *in-situ* crosslinking depending upon the viscosity of the biopolymers (Fig. 2). Low viscous polymers combined with photoinitiators and photochemicals are mostly either pre-crosslinked (pre-crosslinking) or crosslinked during the printing process (*in-situ* crosslinking) whereas high viscous polymers are preferably crosslinked only after the printed process is over (post-crosslinking). Photocrosslinking methods have been successfully used in the fabrication of 3D constructs as *in vitro* models that faithfully recapitulate the complexity of both healthy tissues as well as diseased tissues.

Pre-crosslinking—Irradiation of light before bioink ejection allowing extrusion of pre-crosslinked bioink; Post-crosslinking—Irradiation of light after the bioink ejection or over the printed constructs; *In-situ* crosslinking—Irradiation of light in the photo-capillary lumen or during the bioink ejection process.

To date, the demand for photocrosslinking approaches and photocrosslinkable biomaterials for 3D bioprinting is exponentially increasing and thus forms the concrete basis to offer a comprehensive review on the current progress of their applications in 3D constructs development. This review paper provides the basic insights of photocrosslinking mechanisms with a focus on the considerations of various parameters involved in photocrosslinking reactions such as irradiation time, location, light intensity, and irradiation distance. Further, the applications of photocrosslinking in various bioprinting technologies such as stereolithography, digital light processing (DLP), and extrusion bioprinting are discussed. Photocrosslinkable biomaterials explored for 3D bioprinting are described along with the current progress of this approach. Finally, the challenges in developing

photocrosslinked 3D constructs and future perspectives on the applications of this strategy in 3D bioprinting are briefly highlighted.

2. Photocrosslinkable biomaterials

Photocurable biopolymers possess light-sensitive functional groups, which can be crosslinked upon the illumination of light at a specific wavelength. These polymers have found substantial and wide applications in numerous fields such as electronics, printing resins, surface coatings, biosensors, surgical applications, drug delivery systems, dental implants, and tissue engineering [13,14]. Further, these biopolymers have also extended their biomedical applications in additive manufacturing techniques, where they crosslink instantaneously to develop a three-dimensional construct during or after the printing process [15]. In addition to the presence of photoreactive side groups, these polymeric bioinks used for successful bioprinting process should possess ideal properties such as (i) mechanical property like toughness, elasticity that matches specific target tissue; (ii) good structural integrity to withstand the desired load and (iii) excellent biocompatibility with negligible inflammatory and immunogenic reactions. These bioink materials are conjugated with photoactive functional groups which are sensitive and selective to a set of photocuring parameters [16]. Table 1 shows a comprehensive list of various conjugated polymeric biomaterials, photoinitiators, crosslinking parameters, and developed 3D constructs using bioprinting methods. It is important to note that unreacted photoactive groups and over-illumination of UV light may lower cell viability, cause inflammatory responses and genetic mutations, which may be considered as drawbacks of this technique. Hence, complete removal of these unreacted groups and shorter UV light illumination time can overcome these limitations to obtain stable and biologically active 3D constructs [17]. These biomaterials can be classified as UV crosslinkable and visible light crosslinkable materials based on the maximum absorption wavelength (λ_{\max}) of the photoinitiators.

2.1. UV crosslinkable biomaterials

Most natural polymers such as gelatin, collagen, and alginate have cell-binding motifs facilitating cell adhesion, proliferation, and differentiation process. However, these natural polymers possess poor mechanical stability to be suitable for long-term *in vitro* cultures [32]. For example, gelatin, a denatured form of collagen type I is a fragile, thermosensitive polymer (gel point > 35 °C, although depends on the molecular weight of gelatin) that have a cell-binding motif (RGD) to aid cell adhesion and proliferation for short-term *in vitro* studies [33]. On the contrary, synthetic polymers such as PEG, poly(vinyl alcohol) (PVA), and poly(acrylic acid) (PAA) were found to be easily tailorable using its functional groups making them have properties such as biodegradability, high mechanical strength, cost-effective and clinically relevant. But they lack biocompatibility by exhibiting immunogenic and inflammatory responses which are undesirable for *in vitro* culture studies. In addition, the mechanical strength of these polymers needs to be carefully scrutinized to match with the native tissues [34]. Thus, the introduction of photocrosslinkable functional groups such as acrylate, methyl methacrylate, or glycidyl methacrylate *via* chemical conjugation to natural and synthetic polymers may impart suitable mechanical strength to the final hydrogel 3D constructs without compromising the cell modulatory activities. For

instance, gelatin methacrylate (GelMA), methacrylated hyaluronic acid, pectin methacrylate, poly(ethylene glycol diacrylate) (PEGDA) are some of the most commonly used acrylated UV photocrosslinkable biomaterials, which require suitable UV photoinitiators such as Irgacure or LAP for efficient photocrosslinking [35].

Recently, decellularized ECM (dECM), a natural biomaterial obtained from native tissues has received huge attention owing to its thermal behavior (gelation at physiological temperature) and capability of dynamic interaction with cells thereby providing a native ECM-mimetic microenvironment. However, dECM may cause high immunogenic reactions due to its allogenic origin from various organisms. Hence, it requires a complete and strong decellularization process to remove DNA and other contaminants without affecting its native functionalities [36]. Jang et al., have developed photoactive dECM by conjugating riboflavin (Vitamin B2) and illuminated using UV light of wavelength 370 nm and intensity of 30 mW/cm² for 3 min to initiate photocrosslinking. This step was followed by entropy-driven self-assembly of collagen to produce a grid-patterned, stable, 10 layered 3D construct with high structural integrity when kept in PBS at 37 °C for 30 min. *In vitro* viability of cardiac progenitor cells remains >95% for 24 h in cell-laden dECM hydrogels prepared using riboflavin concentrations up to 0.1%. Further, the prepared 3D hydrogel constructs had higher stiffness (<1 kPa) similar to that of native cardiac tissue. In addition, the quantitative real-time PCR (qPCR) of the printed constructs showed increased expression of cardiac differentiation factors such as cardiac troponin I, myocyte-specific enhancer factor 2C, GATA4, and Nk2 homeobox after 7 days of culture, which confirms the myogenic differentiation of cardiac cells [37].

2.2. Visible light crosslinkable biomaterials

The visible light crosslinking reactions are devoid of phototoxicity and potential mutations thereby promoting higher cell viability and biocompatibility in the printed structures [16]. On the contrary, the use of UV light in the crosslinking process may affect the cytocompatibility of cell-laden hydrogels and lead to cancer and other related ailments in the neighboring tissues, as observed in the intravital crosslinking process (discussed in Section 4.4). Visible light photoinitiators such as Eosin Y, ruthenium (Ru), camphorquinone, and fluorescein have been widely used in biomedical applications, which act as an additive component in the formation of stable hydrogels. However, conjugating visible light photoactive groups in biopolymers have become a recent trend in developing novel visible light crosslinkable biomaterials [38]. Tyrosine with a phenolic functional group is the most commonly used visible light photoinitiation component conjugated with natural or synthetic biopolymers. Generally, irradiation of visible light in the tyrosine tagged biopolymers causes sequential steps such as (i) hydrogen abstraction in the hydroxyl groups of tyrosine (free radical formation); (ii) radical isomerization causing radical recombination of two different tyrosine molecules, and (iii) enolization forming dityrosine bonds between the tyrosine tagged polymers [39]. This type of reaction can also be performed using additive components such as horseradish peroxidase and hydrogen peroxide, iron ions causing Fenton's reaction, ruthenium/sodium persulfate [40,41]. Sakai et al. developed a bioink made of hyaluronic acid and gelatin tagged with phenolic residues, Ru/SPS crosslinking system, and human-derived adipose stem cells (hADSC). The developed bioink was

printed *via* a micro-extrusion process into two different patterns such as hemisphere and three-layered lattice-shaped 3D structure with 0.6 mm thickness and analyzed for its cytocompatibility. After 24 h, the printed cells were rounded and viable and later the cells showed elongated morphology with high metabolic activity after 5 days. In addition, the cells in the bioprinted constructs exhibited upregulation of pluripotent genes such as Nanog, Oct4, Sox-2 and expression of cell surface marker proteins such as CD34 and CD44 [42]. Another study developed a three-component visible light photoinitiator system using carboxylated camphorquinone (CQCOOH), L-arginine (amine coinitiator), and diphenyl iodonium chloride (DPIC, accelerator) mixed with a water-soluble polymer, 2-hydroxyethyl methacrylate conjugated hydroxyethyl starch (HES-HEMA). Irradiation of visible light from LED lamps for about 1.9 min causes the formation of two initiating radicals by CQCOOH and coinitiator molecule. Additional free radicals were formed using accelerator molecules, which involve in the propagation step during the photocrosslinking process. Mechanical analysis of the photocrosslinked gels showed higher storage modulus (10 kPa) when compared to the non-crosslinked solutions (0.5 kPa). *In vitro* seeding of human gingival fibroblasts in the developed three-component, visible light photoinitiator system showed good biocompatibility, which was confirmed by MTT and LDH assays [43].

3. Photo-crosslinking strategies

Biomimetic scaffold fabrication techniques such as electrospinning, solvent casting, gas foaming, and additive manufacturing require biomaterials (bioinks / bioresins) to develop films, fiber mats, and hydrogels with desired properties and cell supportive features [44]. Hydrogels are crosslinked polymeric networks that entrap water and become colloidal gel-containing water as the dispersion medium. These hydrogels can be tailored for various tissue engineering applications using crosslinking strategies such as ionic, enzymatic, chemical and photocrosslinking methods [8] (Fig. 3A). Among these crosslinking techniques, photocrosslinking is an emerging technique in bioprinting applications, where absorption of light energy (such as UV, visible, and IR wavelengths) by the prepolymer molecules induce a photo-chemical reaction, which leads to the formation of covalent bonds between the polymeric chains resulting in stiffer and stable hydrogels. Various photo-crosslinking methods such as free radical polymerization, biorthogonal click reaction, redox-based photo-crosslinking, and their combinational methods are commonly adopted for the conversion of precursor polymers into mechanically stable polymeric hydrogels [11]. This is highly useful in conventional scaffold fabrication and 3D bioprinting applications, particularly for the long-term *in vivo* implantation applications [45,46]. The basic components involved in any photo chemical reactions are precursor polymers, photo initiators, sensitizers, and light energy (Fig. 3B). The basic principles and mechanisms involved in photocrosslinking reactions to fabricate 3D constructs along with their advantages and disadvantages are discussed in subsequent sub-sections.

3.1. Free radical polymerization

Free-radical or chain-growth polymerization involves the production of free radicals upon exposure to incident light and is one of the most common photo-crosslinking strategies for the preparation of hydrogels. This type of reaction generally undergoes three different

stages—initiation, propagation, and termination (Fig. 4). In the initiation step, free radicals (active center) are generated by homolytic photolysis of the initiator molecules, which primarily depends on the light intensity, duration of the incident light, quantum yield, number of free radicals generated per photolytic event, concentration, and efficiency of the photo initiators [47,48]. These generated free radicals in turn react with the non-steric ends of the monomeric units thereby transforming their active centers into pre-polymers (reactive intermediates). In the propagation step, non-reactive monomers react sequentially with these reactive intermediates, thereby leading to the faster growth of polymer chains. In the termination step, these active centers are destructed *via* several methods – (i) by combining the ends of the radical active centers (radical coupling); (ii) by using a chain transfer agent to transfer the radical species away from the propagating chain and (iii) by disproportionation reaction which lead to the formation of one saturated and another unsaturated terminal group [49].

Acrylate and methacrylate derivatives of vinyl-based polymers such as PEGDA, poly(ethylene glycol dimethacrylate) (PEGDMA), and gelatin methacrylate (GELMA) are predominantly used for the synthesis of photo-crosslinked hydrogels using free-radical polymerization in the presence of photo-initiators such as 1-benzoylcyclohexanol, LAP, 2,2'-Azobis [2-methyl-*N*-(2-hydroxyethyl)] propionamide (VA-086) and Irgacure 2959 [50]. Widiyanti et al., have prepared poly(ethylene glycol dimethacrylate)/nano-fibrillated cellulose (PEGDMA/NFC) hydrogels by irradiating UV light at wavelength 366 nm on the precursor solutions containing varying concentrations of PEGDMA and NFC (1:0.25, 1:0.5, 1:0.75) with Irgacure 2959 as photo initiator [51]. Fourier transform infrared spectroscopy (FTIR) analysis of these hydrogels confirmed the presence of CC bonds between the photo-initiator and PEGDMA which confirms the crosslinking reactions. Further, an increase in the concentration of NFC in these hydrogels increases the fibrous morphology with augmented compressive strength (3.42 kPa for 1:0.75 PEGDMA: NFC) and decreased swelling rate (80% for 1:0.75 PEGDMA: NFC) when compared to uncrosslinked PEGDMA hydrogels. In addition, the injectable property of these hydrogels was found to be suitable for the restoration of vertebral disc degenerative disorders. In another study, O'Connell et al. examined the free radical kinetics by illuminating gelatin methacryloyl (GelMA) and Irgacure 2959 as photo-initiator present in DPBS medium using UV light (365 nm). Upon absorption of UV by the photo-initiator, benzyl and ketyl radicals were produced by alpha-cleavage process. These benzyl radicals play a major role in initiation of the polymerization process whereas the ketyl radicals were found to be short lived as they tend to react rapidly with aqueous medium. Moreover, *in-situ* rheological properties of the GelMA irradiated with varying light intensity (2–150 mW/cm²) showed no significant difference in the storage modulus for each tested concentrations, however the crosslinking kinetics increased dramatically when the light intensity was increased. For example, the onset time of gelation for GelMA samples exposed to 2 mW/cm² was 290 s while samples exposed to 150 mW was only 4 s. Importantly, decreasing the photo-initiator concentration and light intensity greatly influence the viability and metabolic activity of the human mesenchymal cells embedded in the GelMA hydrogels [52]. Hence, the choice of photo-crosslinking conditions such as light intensity, photo-initiator concentration, and degree of reactive functional groups in polymers have to be carefully considered during the fabrication of 3D hydrogels.

Hydrogels produced through ideal conditions possess tunable porosity, degradation rate, and mechanical property, which primarily depend on crosslinking density [53]. For instance, the mechanical property and biocompatibility depend on the degree of methacrylation in GelMA [54]. A decrease in crosslinking density due to low methacrylate groups in GelMA leads to the formation of hydrogel with larger pore size and greater swelling behavior which may favor incorporation of biomolecules but hydrogel processability is greatly compromised. These types of crosslinking reactions yield irreversible bond formation and offer several other advantages such as faster conversion rate, aqueous reaction conditions, and higher reactivity of free radicals. On considering these advantageous attributes, these reactions may be suitable for fabricating 3D constructs using an extrusion-based 3D bioprinting process [35]. However, these reactions may result in heterogeneity in working with high molecular weight and highly branched or cyclic polymer backbones, which are caused due to steric hindrance effect of prepolymers, diffusion kinetics of free radicals, and free radical formation in mid-polymer chain length [55]. These limitations may greatly affect the degradation rate of the fabricated 3D structures.

3.2. Bio-orthogonal click reaction

Bio-orthogonal click chemistry is a light-mediated step-growth reaction characterized by orthogonal reactivity of pre-polymers and uniform formation of polymeric networks with minimal defects [56]. Unlike free-radical polymerization, this type of reaction is insensitive to water and oxygen and possesses advantages such as higher efficiency, faster reaction kinetics even at low concentrations, higher binding selectivity under mild or aqueous conditions, and *in vivo* high biocompatibility [57]. Aldehyde/ketone condensation, strain-promoted oxidation-controlled cyclooctyne-1,2-quinone cycloaddition (SPOCQ), cyanobenzothiazole condensation; strain-promoted cycloaddition of azides and alkynes (SPAAC), inverse electron-demand Diels–Alder (IEDDA), hetero-Diels–Alder reactions, 1,3-dipolar cycloadditions, and thiol-norbornene photo-click reactions are some of the biorthogonal reactions used for different applications such as drug discovery, polymer synthesis, material science studies, biomolecular modifications, and nanotechnology [58,59]. Among these, thiol-norbornene photo-click reactions have been predominantly used in the preparation of hydrogels [35]. Thiol-norbornene type of reaction also involves three sequential steps (i) Initiation—Irradiation of photoinitiators *via* light forms radicals, which abstracts protons from thiol group functionalized polymers generating thiyl radicals (ii) Propagation—Thiyl radicals undergo anti-Markovnikov reaction, where they react with electron-rich or strained -enes secondary molecules forming carbon-centered radicals along with intermolecular thioether bonds (Fig. 1) [11]. Rapid addition of polymers results in trimers, oligomers, and eventually longer polymers with a consistent increase in the molecular weight of the formed polymers. Generally, this type of reaction does not terminate and remains active with an active center in the ends or side chains of the polymer [60]. It should also be noted that there is an arguable statement that they can terminate *via* disulfide formation *via* thiyl-thiyl radical coupling [61]. Polymers containing or functionalized with -ene groups such as vinyl ethers, methacrylates, and norbornene are commonly used as precursor components in this type of reaction.

In a study conducted by Pereira et al., a one-pot, photo-crosslinked, and biodegradable pectin-based hydrogels *via* step-growth polymerization through thiol-ene linkages were synthesized. The precursor solutions containing norbornene functionalized pectin macromolecules, VA086 (0.25%), cell adhesive peptide (RGD), and Type I collagen mimicking crosslinker peptide (CGPQG↓IWGQC (4–6 mM, down arrow, denotes cleavage site for matrix metalloproteinases) were irradiated using UV light (365 nm, 7 mW/cm²) for a shorter duration of 20 s to develop photo-crosslinked hydrogels. There was negligible bubble formation due to nitrogen production by VA086 concentration present in the prepolymer solution. The final hydrogel constructs exhibited decreased swelling ratio and increased elastic modulus (446.75 ± 35.66 Pa). Further, crosslinking density was found to be increased in a higher concentration of crosslinker peptide (6 mM) when compared to lower concentrations (4 mM). In addition, matrix metalloproteinases (MMPs) induced degradation assays showed rapid degradation even for highly crosslinked hydrogels yet these gels were found to be structurally stable and intact for the tested period. Hydrogels embedded with human neonatal dermal fibroblasts (hNDFs) showed uniform and elongated morphology of cells in RGD conjugated pectin-based hydrogels irrespective of their crosslinking densities during the 7 days of *in vitro* culture. This was attributed to the space availability in loosely crosslinked hydrogels and MMPs mediated degradation for highly crosslinked hydrogels. To mimic the dermal and epidermal regions of native skin, keratinocytes were seeded on fibroblasts-laden hydrogels after 7 days and co-cultured for one week. This *in vitro* study report confirmed elongated fibroblasts and dense, flattened keratinocytes with proliferative potential and secretion of ECM markers such as Collagen I, Fibronectin, Ki67, and vimentin [62].

Copper-catalyzed SPAAC reactions were one of the oldest click chemistry-based techniques for developing biomaterials, yet had very limited usage in biomedical applications due to the toxicity induced by copper [63]. Hence, copper-free SPAAC reactions were considered to have many advantages such as less cytotoxicity, high specificity, and reactivity, thus best suited for various biomedical applications such as protein labeling, injectable filling materials, and cell-laden hydrogels. Brown et al., developed a three-dimensional muscular scaffold by crosslinking azadibenzocyclooctyne (DBCO) and azide-functionalized poly (ethylene glycol) macromers, which initially yielded a soft hydrogel (SPAAC crosslinking). Subsequently, the addition of LAP as photo-initiator and irradiation of UV light (365 nm, 10 mW/cm²) for 2 min yielded a stiffer hydrogel due to photo-initiated crosslinking of pendant DBCO groups. *In vitro* studies performed on soft (SPAAC alone without photocrosslinking) C2C12 cell-laden hydrogels showed 87% cell viability with native extended morphology after 24 h. On the contrary, photocrosslinked (SPAAC + photocrosslinking on day 1) C2C12 cell-laden hydrogels showed decreased (80%) cell viability, rounded cell morphology, and decreased expression of Yes-associated protein (YAP) after 24 h. Irradiation of UV light on 7-day cultured soft gels resulted in stiffer hydrogels with increased nuclear localization, better expression of YAP, and also displayed extended morphology within the gels that mimic the native muscular environment with tunable mechanical properties [64]. However, biorthogonal *click* chemistry-based reactions possess few constraints such as unstable reactants, cross-reactivity with target molecules, and the limited solubility of reactants.

Hence, careful tuning of parameters such as concentration of reactants and catalysts, temperature, and pH have to be carried out to overcome these limitations [65].

3.3. Redox crosslinking

In this type of photo-crosslinking method, photosensitizers act as light (visible or infrared spectrum) absorbing molecules where they excite and transfer the incident light energy to the neighboring molecules. Upon irradiation of light, these molecules absorb light and excite into a triplet state. Two main reactions might occur during the return of excited photosensitizer to its ground state and production of radicals. (i) Type I reaction—The excited photosensitizer reacts with deoxygenated molecules to form a product and photosensitizer again. (ii) Type II reaction—The excited photosensitizer reacts with ground state triplet oxygen molecules resulting in the quenching of photosensitizer and formation of a singlet state oxygen (typically referred to as Reactive Oxygen Species (ROS)), where it reacts with the substrate to form a product [66] (Fig. 6).

Hong et al. prepared photo-crosslinked tyramine-modified hyaluronic acid (HA/Tyr) hydrogel using Riboflavin (RF) as visible light (440 nm) photosensitizer irradiated for 30 s. These irradiated solutions were left overnight to undergo complete crosslinking of the hydrogels. During this process, phenolic groups of tyramine modified HA reacts with $^3\text{RF}^*$ (excited riboflavin formed after irradiation) through radical coupling. These photocrosslinked hydrogels showed good stability for up to 3 months under dark conditions and also displayed increased storage modulus with an increase in HA concentration [67].

3.4. Dual crosslinking

Low viscous bioinks or polymer solutions particularly in bioprinting applications favor cytocompatibility but remain challenging in the fabrication of stable 3D structures. Therefore, an efficient, fast, and dual crosslinking method is imperative to maintain the shape and size fidelity of the printed structures especially for the long term *in vivo* or *in vitro* studies in tissue engineering applications [68]. The dual crosslinking method can be performed in two ways—first in adding two different photo-initiators in precursor solutions and second in photocrosslinking along with chemical, physical or enzymatic crosslinking methods. Both these methods aim to produce structurally stable hydrogels with desired mechanical strength, particularly for 3D bioprinting of multilayered structures with excellent shape fidelity and superlative bonding between the different layers of the 3D constructs [10] (Table 2).

Han et al. recently developed a photocrosslinkable hydrogel using a dual photo-initiator approach. Here, the pre-gel solution contained PEGDA and photo-initiators such as Irgacure 2959 and VA-086 along with L929 mouse fibroblast cells. This composition was irradiated with UV light (365 nm, $\sim 19 \text{ mW/cm}^2$) specific for VA-086 at low illumination time (2 min). The free radicals generated due to activation of VA-086 induced the activation of Irgacure 2959 to generate more free radicals, which ultimately enhanced crosslinking efficiency of the developed PEGDA hydrogel solution. In addition, cells embedded in a dual photoinitiator system exhibited increased cell viability (90%) when compared to a single photo-initiator system containing Irgacure (30% viability) [76]. Several reports

suggest the use of dual photo-initiators in developing biocompatible, cell-laden polymeric suspensions, microspheres, and hydrogels since it requires low photo-initiator concentrations and provides superior photo-crosslinking efficiency with high product yield [77,78]. Yet another type of dual crosslinking approach involves photo-crosslinking coupled with other crosslinking methods. This hybrid method is one of the widely used approaches for 3D bioprinting applications [10,72] (Table 2). In a study, Soliman et al., utilized allyl functionalized gelatin (Gel-AGE), thiol functionalized DTT or PEG, and visible light photoinitiator Ru/SPS to develop a dual crosslinkable low-density bioinks for extrusion-based bioprinting method. This precursor solution was initially crosslinked by the redox method, where covalent bonds were formed between thiol functionalized DTT or PEG and Gel-AGE. Successively, this solution was irradiated with visible light for 3 min to induce secondary crosslinking *via* thiol-ene based click chemistry reaction. By utilizing this dual crosslinking method, four-layered human articular chondrocytes (HACs) laden constructs were printed and found to have ~90% cell viability for up to 7 days *in vitro*. In addition, rheological analysis of the hydrogels developed with direct (photo-crosslinking alone) and dual crosslinking methods (redox and photo-crosslinking) showed similar compressive strength and also enabled good stability in the printed constructs [79].

4. Design considerations in photo-crosslinking

For a successful photocrosslinking technique to bioprint, viable and functional tissue constructs with better resolution and good stability, certain parameters such as light source, photoinitiators, crosslinking density, crosslinking location and rheological characteristics of the hydrogel needs to be scrutinized [52]. In addition, the interactions between these parameters with the biopolymers and cells and their subsequent influence on construct features need to be understood in great detail. In light of the above, these parameters have been discussed in this section as this technology involves a lot of challenges ranging from optimization of resolution to biocompatibility of the printed structures. Rational choice of these parameters is of paramount importance in the development of stable and effective 3D bioprinted tissue constructs using the photocrosslinking technique.

4.1. Light source

The light source is one of the most important considerations in the photocrosslinking process. Photoinitiators or co-initiators get activated by absorbing specific wavelengths of light, thus the light source should primarily be congruent with the maximum absorption wavelength (λ_{max}) of the photoinitiators and possess the following LASER characteristics such as highly monochromatic, polarized, coherent, collimated with high intensity. Light sources having a wide range of wavelengths may be suitable for an extensive variety of photoinitiators (eg. commercially available UV bulbs) but the light cannot be absorbed by the photoinitiators maximally, which may lead to a poor photo-crosslinking process. Commonly used light sources would fall in UV (UV-A (320–400 nm) and UV-B (290–320 nm)) and visible light (400–700 nm) wavelengths during photocrosslinking, of which UV-C (200–290 nm) ranges are avoided as they are mostly used for germicidal and sterility purposes [80]. Further, the chosen wavelengths and their exposure duration have a direct impact on the viability of the cell-laden hydrogel constructs, in which shorter wavelengths

(eg. UV-B) and longer exposure duration decrease the cell viability of the constructs causing epigenetic or genotypic damage due to unwanted mutations [81]. In addition, UV light has lesser optical penetration depth, which results in uncrosslinked or poorly crosslinked constructs in interior regions of the hydrogels. In contrast, visible light has deeper optical penetration when compared to UV light sources [42]. It was reported that visible light crosslinked hydrogels showed better cell viability and crosslinking ability with higher tissue penetration depth. Lim et al., investigated the cytotoxicity and metabolic activity of the human articular chondrocytes-laden gelatin hydrogels by photocrosslinking using two different UV and visible light sensitive photoinitiators [82]. Further, *in vitro* experiments confirmed that visible light crosslinking had greater penetration depth with homogenous crosslinking throughout the construct, 85% cell viability, higher metabolic activity, and extracellular GAG content with chondrogenic differentiation ability even after 35 days when compared to UV crosslinked hydrogels. Another study also reported that GelMA gels photopolymerized with visible light showed higher viability of KUSA-A1 cells over the culture period of 7 days when compared to gels crosslinked with UV light. Visible light crosslinked GelMA hydrogels also showed higher osteogenic differentiation genes such as Runt-Related Transcription Factor 2 (Runx2), Osterix (Osx), bone sialoprotein (Bsp), and osteocalcin (Ocn) [83].

Few other light source parameters such as light intensity (W/cm^2) and distance between the light and the biomaterial also play an important role in cell viability, gelation kinetics, and mechanical strength of the crosslinked hydrogels [84]. For instance, irradiating large and thicker 3D constructs at a constant distance, the intensity of the light might decrease in the deeper regions when compared to top/superficial layers of the constructs, hence resulting in differential crosslinking kinetics yielding heterogenous porous network throughout the construct.

4.2. Photo-initiators

The selection of photo-initiators is another important criterion for efficient photopolymerization of the developed bioink and allows negligible toxicity during the fabrication of viable 3D cellular constructs [48]. Generally, photo-initiators can be categorized as cationic and free radical systems depending upon the generation of reactant products upon light irradiation (Table 3).

Typically, these generated products involve the polymerization and crosslinking of the polymeric units. Photoinitiators that generate free radicals upon light absorption are termed free radical photoinitiators, which are mostly of styrene or acrylate conjugated aromatic carbonyl compounds [47]. They are classified as Type I and Type II depending upon their photofragmentation during the free radical generation process Type I molecules cleave with a unimolecular reaction to generate free radicals. Generally, the carbonyl group of the photoinitiator absorbs the light to form excited α -carbons, which will undergo homolytic cleavage to generate two free radical fragments. Type II photoinitiators cleave as a bimolecular reaction, where these photoinitiators require a hydrogen donor (synergists) to generate free radicals [93] (Fig. 7).

Cationic photo-initiators include mostly onium salts or organometallic complex salts, which undergo homolytic cleavage similar to Type I photoinitiators but will generate free radicals with strong photoacids such as Lewis or Broensted acids upon absorption of light [94]. These photoacids remain active even after removing light, which may alter the pH thereby affecting the cell viability and considered suitable for cancer-related studies [95] and micro-electronic fabrication [96] but not for tissue regeneration applications. In addition, the light absorption wavelength mostly falls in the deep UV range, which may be cytotoxic to the cells [97]. Some of the commercially available and commonly used photoinitiators and their properties were listed in Table 4.

These photoinitiators were chosen based on certain ruling parameters such as maximum absorption wavelength (λ_{\max}) of photo-initiators, several quanta of photons absorbed by photoinitiator, quantum yield (ϕ), photobleaching ability, concentration, solubility and cytotoxicity in physiological conditions, light exposure duration and chosen cell type [48,98]. Many reports are supporting how these parameters have a direct impact on the viability of the bulk or patterned cell-laden constructs [93,99]. Xu et al. compared the cytocompatibility of two different commercially available photoinitiators such as Irgacure 2959 and LAP in Human Umbilical Vein Endothelial Cell (HUVEC) laden 3D printed gelatin methacrylate (GelMA) based constructs. It was suggested that a lower concentration of photoinitiators showed good cellular viability in the printed constructs whereas, at higher concentrations, LAP crosslinked constructs showed good viability than Irgacure 2959 crosslinked constructs during the bioprinting process. In addition, Irgacure 2959 crosslinked GelMA constructs showed poor mechanical property with a faster degradation rate and higher pore size when compared to LAP crosslinked constructs [100].

Another crucial parameter that needs to be considered is oxygen inhibition. Oxygen inhibition occurs due to the interactions of the free radicals (generated by photolysis of photoinitiators) with the molecular or atmospheric oxygen (O_2) that are present *in vitro* or *in vivo* conditions [101, 102]. These oxygen molecules may hinder the kinetics of the photolytic reactions in several ways—(1) Exited photoinitiators formed by absorption of light may get quenched (2) The free radicals generated in the initiation/propagation steps during the polymerization process react with the O_2 molecules at a rate constant of 10^6 times higher than that of the propagation step, which lead to the formation of peroxy radicals [49] (3) These peroxy radicals may terminate the polymerization process *via* radical-radical coupling mechanism or hydrogen abstraction from an adjacent molecule forming a new radical with poor reactivity towards photocrosslinkable functional groups [101,103]. Further, these peroxy radicals act as a good oxidizing agent causing a reduction in the formation of free radicals and eventually affecting the rate of photopolymerization. In addition, these peroxy radicals scavenge and hinder the reaction of free radicals with functional groups such as acryloyl and methacryloyl groups, which are the most common photocrosslinkable groups present in the biopolymers leading to partial or incomplete crosslinking of the hydrogels [101].

There are several strategies to suppress the effect of oxygen inhibition—(i) By increasing the photoinitiator concentration and light intensity to generate more free radicals than the available oxygen species, (ii) By introducing chemical species or additives such as

amines, *N*-vinyl amines, silanes, thiols, boranes, phosphines and phosphates, ethers and (iii) By removing the oxygen species by degassing or curing in an inert gas (N₂, Ar, CO₂) atmosphere [104]. Although these approaches may control the oxygen inhibition process, these methods have several limitations and also may alter the basic requirements of *in vitro* conditions such as pH and other vital parameters. For instance, introducing thiol or amine groups may develop odor and change the color of the photocrosslinked structures. Likewise, the use of high-intensity light for curing may cause damage to the cells and biological moieties present in the photocrosslinking environment [102].

Some photoinitiators like eosin Y may require the addition of amine-based compounds as co-initiators or sensitizer molecules for the abundant production of free radicals. These amine-based co-initiators were found to be toxic, carcinogenic, alter mechanical properties, and turn the color of the hydrogels or printed construct to yellow. However, undesirable features may depend upon the concentration of co-initiators [105,106]. Camp et al., developed an efficient method for preparing a dityrosine based photocrosslinked hydrogel using elastin-like polypeptides (ELP) with tyrosine residues as biopolymer, tris(2,2'-bipyridyl)ruthenium(II) ([Ru(II) bpy₃]²⁺) as photoinitiator and ammonium persulphate (APS) as coinitiator and oxidizing agent. ELP polymer crosslinking occurs as a systematic reaction steps—(i) excitation of [Ru(II)bpy₃]²⁺ by absorption of visible light, followed by reduction of persulphate anions; (ii) Reduced persulphate anions decompose into sulfate radicals and sulfate anions and (iii) Excited [Ru(II)bpy₃]²⁺ reduces the tyrosine phenyl groups present in ELP to form radicals that spontaneously dimerization resulting in stable crosslinked hydrogels. However, the use of APS and [Ru(II)bpy₃]²⁺ in biomedical applications might have an impact on its cytocompatibility with cells. Hence, the authors have examined the cytocompatibility of these compounds at various concentrations. The results showed that use of a low concentration of APS (15 mM) along with [Ru(II)bpy₃]²⁺ (up to 125 μM) in an ELP (Tyr) based construct resulted in less or no cytotoxicity of fibroblast cells when irradiated for 10 min using visible light with wavelength 460 nm when compared to a higher concentration of APS irrespective of Ru concentrations. In addition, elastic moduli of these hydrogels can be modulated according to APS and Ru concentrations and mimic the mechanical strength of native tissues [107].

4.3. Rheological characteristics

Crosslinking the polymers with various concentrations of photoinitiators or co-initiators or the addition of hybrid materials such as nanocomposites would eventually affect the mechanical strength of the final printed or bulk hydrogel in terms of its elasticity, stiffness, compressive strength, and viscosity. These will in turn influence the physical parameters such as porosity, pore size, swelling rate, degradation rate, and stability of the developed hydrogel constructs. Bochove et al., have prepared 1 mm thick, flexible poly(trimethylene carbonate) (PTMC) films using particulate leaching and stereolithography (SLA) method. In the SLA method, PTMC films were photocrosslinked using ethyl(2,4,6-trimethyl benzoyl) phenyl phosphinate (TPO-L), type I photoinitiator, and Orasol orange dye at 365 nm for 30 min. In particulate leached films, porogen (NaCl) and unwanted reactants were removed by immersing in ethanol and water for about 1 week. Results concluded that photocrosslinked PTMC films exhibited higher elastic moduli, tensile strength, and toughness when compared

to particulate leached PTMC films. In addition, an increase in crosslinker concentration and a decrease in porogen concentration resulted in porous films with lesser porosity and *vice-versa* [108]. Generally, a lesser crosslinking density of the polymers results in higher pore size with better cellular migration properties. However, the poor mechanical stability of these crosslinked hydrogels with faster degradation *in vivo* conditions was obtained [109]. Additionally, increased crosslinking density led to stiffer and decreased pore-sized hydrogels, which will affect the cell migration ability within the gels. Thus, the careful scrutinization of crosslinking density of the polymers has to be performed to obtain an optimized porosity ratio, degradation, and swelling rate required for specific tissue engineering applications. Many reports are suggesting the importance of porosity with crosslinking density with the mechanical strength of the developed hydrogels to maintain a balanced crosslinking density for sustained cell growth and proliferation.

In another study by Shin et al., a bioink was developed using decellularized extracellular matrix derived from porcine cardiac tissues mixed with laponite-XLG nanoclay, and PEGDA. This developed bioink exhibited viscoelastic behavior with high yield stress ($\sigma_y >$ critical σ_y), which indicates good stackability and shape fidelity for the printed constructs. The addition of laponite in the bioink increases the viscosity of the solution and supported solution printability. Further, the prepared bioink was printed as an 18 layered square-shaped (10 × 10 mm) 3D construct using extrusion bioprinting technique and then irradiated at 405 nm for 30 s. Altering the concentrations of PEGDA (photoinitiator) resulted in varied compressive moduli that matched with native tissue ranging from healthy cardiac tissues (5–15 kPa) to fibrotic tissues (30–100 kPa). Further, *in vitro* studies of the developed bioink with various cells such as human cardiac fibroblasts (HCFs), human induced pluripotent stem cell (hiPSC) derived cardiomyocytes, and human bone marrow-derived stromal cells (HS27A) to fabricate an engineered cardiac tissue (ECTs) resulted in good biocompatibility (>90% viability) within the printed constructs for about 7 days [110]. Xu et al., have developed an ideal tracheal substitute to treat long segmental defects of the trachea using decellularized trachea matrix (DTM) prepared using laser micropore technique (LMT). This resultant matrix LDTM matrix was added with o-nitrobenzyl derivative grafted hyaluronic acid (HA-NB), gelatin, and auricular chondrocytes to fabricate tubular constructs. Then, the prepared bioink was irradiated using UV light (365 nm) for 2 min. Further, rheological analysis of the photocrosslinked hydrogels displayed higher storage modulus (1000 Pa) and compressive modulus (500 kPa), which indicates efficient photocuring property. Moreover, *in vitro* culture of chondrocytes laden photocrosslinked LDTM bioink showed good viability, proliferative ability, and increased DNA content within the printed constructs for about 7 days. Finally, subcutaneous implantation of these hydrogels in nude mice had demonstrated successful maturation into cartilage tissue similar to native cartilage after 12 weeks of surgery [111].

4.4. Photocrosslinking stages

Limitations in incident light penetration into internal regions of thicker hydrogels may lead to incomplete crosslinking or heterogenous crosslinking. To overcome these penetration limits, higher intensity of light or longer exposure time is required for complete crosslinking of the hydrogels [52]. This may severely impact the viability and functionality of the

cells. As an alternative, homogenous crosslinking could be achieved by using additive manufacturing technology where hydrogel bioinks are printed and crosslinked in a layer-by-layer manner (post crosslinking). Especially, this strategy would be beneficial for low viscous bioinks to obtain a stable 3D construct with good shape fidelity. This type of crosslinking is widely used in extrusion and ink-jet-based bioprinting methods [56,71,112]. In addition, increasing the concentration of the bioinks by adding viscosity enhancers such as methylcellulose or nanocomposites might result in higher shear stress and also create a clog in the nozzles during the extrusion process, which affects the viability of the extruded cells [185]. Kim et al., synthesized a tyramine modified poly (γ -glutamic acid) (γ -PGA-Tyr) polymer via *N*-(3-dimethyl aminopropyl)-*N'*-ethyl carbodiimide hydrochloride-*N*-hydroxysuccinimide (EDC-NHS) chemistry forming an amide bond between the carboxylic group of γ -PGA and the amino group of Tyramine. Further, γ -PGA-Tyr was photocrosslinked by the addition of a photoinitiator (Ru^{2+}) and co-initiator (sodium persulphate). It was observed that the crosslinked hydrogel showed an increase in compressive modulus and strength with an increase in irradiation time. Moreover, these hydrogels exhibited good cytocompatibility when cultured with NIH3 T3 fibroblasts for up to 5 days. The prepared bioink can also be blended with natural polymers to enhance its printability and cell adhesion properties. For instance, the γ -PGA-Tyr polymer was blended with hyaluronic acid (HA), methylcellulose (MC), alginate acid (Alg), and cellulose nanofibrils (CNF). These blend bioinks were extruded into 3D lattice structures with dimensions $20 \times 20 \times 2$ mm using the pneumatic-based extrusion bioprinting technique. Then, the printed constructs were irradiated using visible light with a wavelength of 454 nm, the distance at 5 cm, and power density at 1.2 W/cm^2 for about 1 min to obtain stable photocrosslinked 3D structures [113]. Photocurable chitosan-based hybrid hydrogels were developed using methacrylate conjugated chitosan (CHIMA), acryl amide (AM) & photoinitiator (Irgacure 2959/LAP), which showed highly porous interconnected structures and significant swellability. These hydrogels also exhibited an enhanced compressive strength (345 Pa) when compared to pristine prepolymers such as CHIMA and AM. In addition, the gelation of 100 μm thick hydrogels mixed with 0.2 wt% I2959 and 0.2 wt% LAP occurred in 30 s and 5 s respectively, when irradiated using UV wavelengths (365 nm & 405 nm) making it suitable for DLP technology. Further, this bioink was printed into various 3D models such as external nose, ear auricle with helical fold, and 3D lattice structures with different sized grid patterns. Biocompatibility tests of these hydrogels with human umbilical vein endothelial cells (HUVECs) showed negligible cytotoxicity and promoted cellular adhesion and proliferation for up to 5 days, which was confirmed using Live/Dead staining and MTT assay [114]. Many reports are signifying the importance of post crosslinking of the printed hydrogels in regenerative medicine applications as they possess remarkable advantages such as the use of low viscous bioinks, limited cytotoxicity, and compatibility of crosslinking agents even *in vivo* conditions [115,116]. Contrarily, the use of pre-photocrosslinked bioinks as adopted for several pre-ionic crosslinked bioinks would be an ineffective method as it results in heterogenous crosslinking of the hydrogels with improper shape and resolution, which causes clogging of the needle during the extrusion-based bioprinting process and creates inconsistent ejection force of droplets during inkjet bioprinting process [38,117].

In-situ crosslinking is another strategy for crosslinking the low viscous bioinks, where light irradiation occurs before the onset of bioink extrusion *i.e.* within the capillary/needle region [118]. This type of crosslinking produces a stable extrudable hydrogel filament to fabricate 3D constructs of any desired shape and size. Further, this method does not require a postcrosslinking step or the use of any viscosity modifiers, thus offering a single-step crosslinking or printing procedure. Galarraga et al. developed a low viscous bioink composed of pendant norbornene functionalized hyaluronic acid, LAP, and DTT, which was directly photocured in the photo-permeable capillary using visible light (400–500 nm) *via* thiol-ene linkages. After the photocrosslinking process, the rheology of the synthesized bioink showed an enormous increase in its storage modulus (G') when compared to the non-crosslinked polymers. *In vitro* culture of primary juvenile bovine mesenchymal stromal cell-laden NorHA printed hydrogels for up to 7 days displayed good cell viability and uniform distribution of cells within the printed constructs with an average cell density of 750–820 cells/mm², which was validated by counting the number of cells at randomly chosen regions (top, middle & bottom). In addition, the cell-laden bioink printed in the form of discs were cultured for up to 56 days and demonstrated the presence of chondrogenic expression markers such as type II-collagen (COLII), aggrecan (ACAN), and SOX9. Further, collagen and glycosaminoglycans (GAG) contents were found to be increased which confirmed the formation of neocartilage tissue [118]. Recently, O'Connell et al., developed *in-situ* crosslinked gelatin-methacryloyl (GelMA) hydrogel using a hand-held coaxial extrusion-based printing system with LED of wavelength 405 nm. Addition of pristine gelatin (3%), photoinitiator—LAP, and viscosity enhancer (1% hyaluronic acid (HA)) to 10% GelMA solution allows the ink to be non-phase separable, crosslinkable, and printable. After photo exposure for 50 s, this GelMA bioink showed increased rheological parameters such as storage and compressive modulus (~40 kPa). *In-situ* photocrosslinking of these hydrogels *via* a hand-held device showed minimum onset of gelation time (0.2 s) with a light exposure duration of 1 s. Further, *in-situ* photocrosslinking of SaOS-2 cell-laden bioink *via* extrusionbased system had demonstrated good printability with ~80% cell viability in core and shell regions of the printed filaments immediately after the photocrosslinking process [119].

As an alternative to other types of photocrosslinking stages, intravital photocrosslinking is another minimally invasive technique with the advantage of crosslinking the injected photosensitive polymers directly into the target tissues/organs of organisms. In general, photosensitive polymers, photoinitiators, and co-initiators are initially blended with or without cells and then injected into the injured site. Immediately, the injection site is exposed to light illumination at a specific wavelength for complete crosslinking of the polymers [120]. However, illumination of UV light (for hydrogels containing UV-based photoinitiators) might be deleterious both to the injected and neighboring cells at the tissue site [93]. Hence, the use of photoinitiators with absorption wavelengths greater than 385 nm (eg. visible light and infrared wavelengths) might be advantageous due to its higher tissue penetration depth, minimal cell damage, and cytocompatibility [121]. Most SLA-based printers for this type of crosslinking have utilized visible light illuminators for applications in the biomedical field. Considering this fact, novel visible light photoinitiators such as cinnamic-based, coumarin-based, carbohydrate-based, and thiol-ene based derivatives need

to be developed to improve this technique for advanced and widespread applications. Recently, Urciuolo et al., developed injectable hydrogel comprising of coumarin-based photoreactive polymers such as 7-hydroxycoumarin-3-carboxylic acid conjugated 4-arm poly(ethylene glycol) (HCC—4-arm PEG), 7-hydroxycoumarin-3-carboxylic acid conjugated 8-arm poly(ethylene glycol) (HCC-8-arm PEG), and 7-hydroxycoumarin-3-carboxylic acid conjugated gelatin (HCC–gelatin). This composition was injected into different sites such as epidermal regions of the abdomen, ear, epimysial muscles of the lateral hind limb, and submeningeal regions of the brain of both inbred (C57BL/6J strain) and transgenic (C57BL/6-(ACTB-EGFP)/J) mice models. This inter-tissue injection was then followed by illumination of near-infrared light (writing duration varies from 1.14 to 5.69 ms/line) with low laser power. After illumination, dimerization of HCC molecules occurs causing coumarin mediated cycloaddition-based crosslinking of hydrogels to stabilize precise and spatially controlled 3D structures within the injected areas. Further, these hydrogels showed excellent biocompatibility with negligible inflammation and cell damage in and around the illuminated regions, which was confirmed using immunofluorescent analysis, histological analysis and absence of cell death markers such as caspases after 4 days. Moreover, injecting mCherry tagged fibroblasts laden HCC-gelatin in epimysial regions of immunocompetent mice showed presence of rounded cell clusters whereas intravitally bioprinting of these cell laden HCC-gelatin solutions showed parallelepiped-shaped constructs within 21 days, which confirmed the compatibility of this technique towards localized delivery of cells. In addition, GFP tagged MuSC- and mCherry tagged fibroblast-laden HCC–gelatin solutions were intravitally printed and analyzed for the cellular arrangement and regenerative ability. Interestingly, it was found that mCherry tagged fibroblast cells were surrounded by GFP tagged MuSCs (*de novo* muscle tissue formation) with striated myotubes and neovascularization similar to native muscle tissue arrangement, which was confirmed by confocal images [120]. Another study by Seo et al. synthesized an injectable hydrogel made of hydroxybutyl methacrylated chitosan (HBC-MA), Eosin Y as photoinitiator, and triethanolamine (TEOA) and 1-vinyl-2-pyrrolidinone (NVP) as co-initiators. This unique composition possessed both thermoresponsive and photopolymerizable properties when subjected to physiological temperature and specific light illumination. Further, *in vitro* studies using these hydrogels seeded with NIH3T3 fibroblasts displayed good cell viability (>90%) and the proliferative ability for up to 72 h. Subcutaneous injection of HBC-MA solutions induced immediate crosslinking due to its thermoresponsiveness at 37 °C and subsequent illumination of visible light (450–550 nm) over the injected skin area further promoted the crosslinking and increased the mechanical stability of the crosslinked gels *in vivo*. Thus, this kind of strategy can be applied for a wide variety of *in vivo* applications such as drug delivery, tissue regeneration, and biosensing applications [72].

5. Photo-crosslinking in 3D printing and 3D bioprinting technology

Three-dimensional (3D) printing is one of the emerging technologies in additive manufacturing to develop 3D objects or living biological constructs in a layer-by-layer manner using computer-aided designing software like CAD & CAM. Several materials including plastics, composites polymers, and cell embedded biopolymers are used as

printing inks that act as scaffold matrices for cells to proliferate and mature into functional tissues. 3D printing techniques utilize acellular biopolymer-based inks such as PCL, PLA, poly(urethane) (PU), PAA, and PVA in the form of pristine polymers or solvent-based polymeric resins [122]. These polymers can be printed at high temperatures along with or without photocrosslinking steps to fabricate 3D structures with precise size and shape. However, controllability in cell seeding and cell distribution in these printed remain very challenging [123]. To overcome this limitation, 3D bioprinting is employed, which is a method to print viable cell-laden constructs with other biologics (growth factors and cytokines). 3D bioprinting offers robust techniques to print different cell types simultaneously and also with desired distribution of cells homogeneously throughout the 3D construct [187]. Most of the 3D printing and bioprinting techniques such as FDM, SLA, SLS, ink-jet, and extrusion-based bioprinting techniques have leveraged the photocrosslinking approach in developing viable 3D constructs [124]. However, few techniques such as LASER-based bioprinting (LIFT, MAPLE-DW, LGDW) have not yet been exploited for 3D printing of biological constructs using photocrosslinking methods. Based on the current advances, this section comprehensively describes the photocrosslinking methods utilized in various printing techniques along with their merits and demerits.

5.1. Stereolithography based printing

Stereolithography (SLA) based printing is one of the widely used nozzle-free techniques to print 3D structures in a layer-by-layer manner. In this technique, photosensitive liquid monomers or oligomers are allowed to polymerize into solid 3D structures upon focused low-power lasers irradiation with controlled intensities using digital micromirror arrays [88]. This technique produces highly precise 3D structures from a wide variety of polymers with well-defined intricate features. SLA-based printing can be classified into mask-less or conventional SLA, mask-based SLA, and laser-based SLA, based on the target light source used for crosslinking. Conventional SLA focuses light directly onto the photopolymer resins and crosslinks the resins wherever the light falls that eventually develop into 3D objects [125]. The mask-based SLA technique uses a photomask in its light path so that the light is allowed to crosslink only in the non-masked regions. This technique has several advantages such as high printing speed with good resolution, precise crosslinking. as that of conventional SLA [126]. However, these techniques have not been utilized for biomedical applications due to complex multi-step processes and the requirement of deep technical expertise [127]. Laser-based SLA is another 3D printing technique that uses lasers as a light source and performs irradiation based on the XYZ movement of the lens to transfer the desired patterns [128]. In this method, biocompatible oligomers with acrylate and methacrylate functional groups and their derivatives are commonly used as photosensitive resins for the fabrication of constructs with desired properties and geometries. Moreover, the ideal requirements of these resins to be utilized for any biomedical applications are similar to the polymers for biomaterial scaffolds such as excellent bioactivity, biodegradability, noncytotoxic, non-immunogenic with desired mechanical and physiological properties mimicking the native tissues [129,130].

Most of the SLA-based printers use UV lasers due to advantages such as cost-effectiveness, the release of low volatile organic compounds, robustness, slow process resulting in

constructs with higher cell viability (90%) and better resolution [131]. However, the printing duration depends on the thickness of the construct and the same time duration is taken for the printing of each layer. UV lasers are prone to generate heat, odor and cause disruptive DNA damage leading to various types of cancers [132]. In consideration of these facts, Wang et al. developed a low-cost visible light-based stereolithography bioprinter assembled with a commercial beam projector. Here, the light source was kept 10 cm away from the printing substrate to induce crosslinking process. In addition, a 4 cm thick infrared (IR) water filter was kept near the light source to eliminate infra-red radiation. By using this printer, three different patterns such as the University of British Columbia (UBC) logo, mesh pattern with varied line widths, and mesh pattern with uniform line width were printed with bioink composed of PEGDA, gelatin methacrylate (GelMA), NIH-NIH-3 T3 fibroblasts and eosin Y as photoinitiator, which were kept in the printing Petri dish (substrate). After photocrosslinking, these hydrogel patterns showed higher porosity with 50 μm pore size, good mechanical strength (Young's modulus—60 kPa), and swelling ability. Further, the printed patterns were printed with good resolution and showed ~85% cell viability for at least 5 days [88]. Natural polymers such as gelatin and collagen can readily form hydrogels due to their thermoresponsive property [133]. However, 3D constructs developed using these polymers in very low concentrations will have poor stability. To overcome this limitation, the addition of other polymers such as PCL, PEG, and cellulose can be performed to enhance the viscosity of these resins. Considering this advantage, blends of natural and synthetic polymers are mostly used as hybrid photoactive resins to provide good cell attachment properties and enhance the viscosity of the resins. In this context, Elomaa et al. developed a hybrid resin made of gelatin methacrylate (GelMA), *star*-shaped poly(*e*-caprolactone) methacrylate (PCL-MA), formamide as solvent & photoinitiator. This developed hybrid photosensitive resin showed desirable viscosity for printing at 32 $^{\circ}\text{C}$, hydrophilicity, swelling ability, and printing fidelity when compared to the pristine polymers—GelMA and PCL-MA. In addition, the culture of human epithelial colorectal adenocarcinoma cells (Caco2) on 3D printed hybrid films demonstrated cytocompatibility and higher cell proliferation for 7 days. Furthermore, these resins were also printed into intestinal villi structures to prove their suitability as scaffolds using the SLA printing technique (Fig. 8) [134]. Based on the initiation step in the photo-polymerization process namely light excitation and photoinitiator absorption, SLA-based printing is classified into two types - single and multiphoton stereolithography. Notably, both these methods have similar propagation and termination steps during crosslinking process.

5.1.1. Single-photon stereolithography—In this type, photoinitiators undergo single-photon linear absorption which acts as a driving force for the polymerization process. Among different methods, mask-based UV light stereolithography and direct laser writing stereolithography utilize single-photon SLA for biomedical applications. However, inadequate depth of light penetration beneath the polymerized layer is a major bottleneck in this type [135]. In a study, Mochi et al. employed direct laser writing SLA equipped with low power blue diode laser (448 nm) as a light source to fabricate 3D constructs from low molecular weight PEGDA and Irgacure 819 as the photoinitiator. Here, the use of low intensity and low power laser caused a reduction in the penetration depth of light by five times, which led to maximum control over intricate features present in vertical or

lateral orientations of the printed PEGDA based 3D structures [136]. Alternatively, physical or digital photomasks (as in mask-based SLA) are developed through microfabrication techniques that control the light exposure and printing duration as they cure the entire 2D cross-section of the 3D model in a single exposure [137]. However, poor quality of photomasks may cause off focal polymerization in the resins, which may affect the resolution of the printed structures.

5.1.2. Multiphoton stereolithography—Multiphoton stereolithography involves the initiation step with the absorption of very few low-intensity photons simultaneously or sequentially to get high-energy radicals using an ultra-short high-intensity laser pulse. Generally, two-photon polymerization stereolithography (TPP-SLA) with Ti: Sapphire femtosecond lasers are the most common method used for regenerative and biomedical applications [138]. Unlike single-photon SLA causing off focal polymerization, TPP works based on nonlinear optical absorption using high intense lasers [139]. Using this method, higher-resolution objects are obtained by fine-tuning the exposure time, scanning speed using manual or digital adjustment of a mechanical shutter in laser pin hole and scanner movement [140]. In this case, the use of a highly sensitive photo-initiator minimizes the light exposure time but also decreases the number of radical generations, though sufficient enough for improving the printing resolution. Farsari et al., have demonstrated the use of two-photon polymerization (TPP) in photocrosslinking the acrylate composite sensitized with eosin Y photoinitiator using a femtosecond laser (1028 nm). This study resulted in the fabrication of 3D structures with 1 μm resolution without any issues of construct shrinkage [141]. SLA-based printing has been employed for printing smaller, complex 3D structures with high dimensional accuracy and excellent surface quality. However, the use of SLA in bioprinting applications has been limited due to downsides such as the need for high-intensity UV lasers for crosslinking purposes and the requirement of time-consuming post-processing steps to remove the support structures, which may affect the biological components present in the printed constructs [142]. Other drawbacks include the high cost of lasers, small build volume, less control over photocrosslinking process, more wastage of source materials, and fragile parts with considerable odor and toxicity. In addition, very few materials such as acryloyl or alkenyl-based biopolymers are currently available for SLA-based bioprinting, thus necessitates the demand for the development of novel biopolymers towards these applications [143].

5.2. Digital light processing (DLP)

Unlike SLA, digital light processing utilizes low-cost UV light that gets ejected from the projector and focused onto photopolymeric resin using rotating mirrors in a digital micromirror device (DMD). Advantageously, this method aids in crosslinking the entire area of focus at one stretch than crosslinking at every single spot. Thus, this technique produces larger and smaller intricate 3D objects in a shorter duration. However, the printing resolution primarily depends upon the number of rotating mirrors and their focusing planes in DMD [144]. Further, this technique has been implemented for printing biocompatible low viscous materials to develop live constructs with desired mechanical stability and shape fidelity. For instance, Kim et al., photocrosslinked hydrogels prepared from glycidyl methacrylate functionalized silk fibroin (Sil-MA) with LAP (photoinitiator) using DLP based techniques

(Fig. 9). These printed hydrogel constructs exhibited enhanced compressive modulus and well-interconnected porosity when compared to the pristine Sil-MA hydrogels. Further, 30% Sil-MA gels possessed appropriate viscosity and demonstrated the high viability of chondrocytes *in vitro* [145].

Table 5 lists the recent literature on the development of 3D constructs using DLP-based 3D bioprinting.

DLP-based printing also possesses disadvantages similar to SLA, hindering its use in clinical applications. The major drawbacks of DLP based printing are (i) Printed parts develop strong odor as it melts the acrylate functionalized pre-polymer and photoinitiator in resin/ink during the printing process which may cause side effects such as headaches and respiratory problems, (ii) The choice of material used is limited only to photosensitive polymeric inks. Further, these polymeric ink materials need to be combined or chemically modified using photoactive functional groups along with photoinitiator, which may be toxic to the cells when used in inappropriate concentrations, (iii) Printing process requires the use of liquid resins/bioinks in large quantity that in turn increase the material wastage during printing and the cost of the printed product [154].

5.3. Ink-jet bioprinting

Inkjet bioprinting is a non-contact printing method as the dispensing head does not contact the substrate. Inkjet printers require less viscous bioink to eject the materials as droplets through either thermal or piezoelectric-based print heads with a printing resolution of 20–100 μm [155]. Thermal inkjet bioprinter uses electric or thermal energy to heat the nozzles to 300 °C for 2 μs that eventually form air bubbles to eject the bioink [156]. In a piezoelectric-based inkjet printer, the applied voltage will create changes in the shape of the piezoelectric material, leading to the formation of droplets [157]. Inkjet bioprinters have several advantages, such as low cost, high print speed, and the feasibility of printing different cell types in a single construct to fabricate complex tissue types. Biocompatible polymers, cells, and proteins such as biotin, endothelial cells, smooth muscle cells [158], *Escherichia coli* [159], stem cells [160], chondrocytes [161] have been printed successfully through the ink-jet printing process. Gao et al. had fabricated mechanically strong cylindrical tissue construct with a dimension of 4 mm diameter and 4 mm height using ink-jet bioprinting technique. The bioink is comprised of bone marrow-derived human mesenchymal stem cells (hBMSCs), photoinitiator (Irgacure 2959), poly (ethylene glycol) dimethacrylate (PEGDMA), and gelatin methacrylate (GelMA). The bioprinted cylindrical constructs showed the homogenous distribution of cells throughout the construct with >80% survival rate. Further, PEGDMA concentration was varied to tune the compressive modulus of the construct. The presence of GelMA in the bioprinted constructs had extensively promoted the osteogenic/chondrogenic differentiation potential of hMSCs. The differentiation study results revealed increased expression of osteogenic gene markers such as RUNX2, DLX5, ALPL, IBSP & BGLAP and chondrogenic markers such as COL1A1, COL2A1, ACAN, COL10A1 & MMP13 after 21 days. These results have confirmed that the developed bioinks and printing method allowed the osteogenic and chondrogenic differentiation of hMSCs. [160]. In another study, human auricular chondrocytes mixed with

PEGDMA and Irgacure 2959 was bioprinted using inkjet printer on a cylindrical mold with 4 mm diameter. These printed constructs were then irradiated with UV light at a distance of 1–2 mm and cultured *in vitro* with and without the addition of growth factors such as FGF-2 and TGF- β 1. Addition of FGF-2/TGF- β 1 resulted in excellent viability ($84.9 \pm 2.2\%$) and proliferation (40% increase) of chondrocytes when compared to constructs cultured without FGF-2 and TGF- β 1. Further, supplementation of growth factors also increased the ECM production and higher expression of chondrogenic markers such as collagen type II, and aggrecan at week 4, indicating the recapitulation of native chondrocyte architecture and functionality [161]. However, inherent disadvantages of inkjet bioprinting such as discontinuous flow of bioink due to cell sedimentation, process difficulties in developing longer/taller structures, clogging issues while printing, and use of low cell densities have limited its extensive use towards biomedical applications [162].

5.4. Extrusion based bioprinting

Among various bioprinting techniques, extrusion bioprinting is considered the most commonly used additive manufacturing technology in the 3D bioprinting technique. In this method, the bioinks are selectively extruded or dispensed from the cartridge through an orifice or nozzle with the help of different forces such as air pressure (pneumatic actuated), vertical and rotational mechanical forces (piston or screw-driven) [186,188]. In these bioprinters, the dispenser unit and collector unit have to be robotically controlled by software to ensure that the extruded filaments are precisely deposited to create 3D structures [163]. Careful consideration of the printing parameters such as bioink viscosity and pH, dispenser force, movement of both dispenser and collector would effectively help in the development of larger 3D constructs with heterogeneous cell types in a shorter fabrication time. Diamantides et al., studied the correlation between the rheological properties and printing ability of the naturally-derived collagen polymer when photocrosslinked with riboflavin (RF) photoinitiator. This bioink was printed using an extrusion-based 3D printer with a temperature-controlled printing bed. Further, these bioinks were printed into dots of different volumes (0.01–0.1 mL) on the print bed at 37 °C. After printing, the deposited collagen dots were exposed to a blue LED (1200 mW/cm²) for 10 s from the beginning of droplet dispensing from the nozzle. Photocrosslinking collagen at various concentrations with RF resulted in higher storage moduli, however higher concentrations of collagen did not yield a significant increase in its storage modulus. Since collagen tends to form fibrous networks of hydrogels at higher pH due to electrostatic and hydrophobic forces between the neighboring collagen molecules [164]. Further, the printing of the bovine chondrocytes-laden collagen bioinks was carried out at different pH and examined for its printing fidelity and cell viability. Results have shown that filaments printed at higher pH exhibited good printing fidelity and the cell viability was not affected with different pH conditions [165].

Extrusion-based bioprinters with multiple print heads have also been adopted to print heterogeneous 3D constructs using various biomaterials and cells. Liu et al., developed a pneumatic-based, rapidly extruding multi-material bioprinter which possesses a single print head connected by seven software-controlled, switchable, and uniform sized capillaries to extrude seven different materials [166]. Bioinks having shear thinning properties such as alginate, gelatin methacrylate, poly(ethylene glycol diacrylate), pluronic, and their mixtures

were allowed to extrude and print human organoids such as brain, blood vessels in the lung, left atrium of heart, liver, kidneys, pancreas, gastrointestinal system and bladder. In addition, other free-form shapes such as coils, double-layered hollow tubes, and DNA helical shape constructs were printed using PEGDA/alginate/pluronic bioink followed by photocrosslinking to yield stable constructs. This strategy resulted in the successful development of micro-fibrous constructs with well-defined spatial architecture and robust (15×) resolution when compared to existing multi-nozzle-based techniques. In another study, Byambaa et al., utilized extrusion-based direct writing method to fabricate bone mimetic constructs with native vasculature. Here, the bioink composition had Irgacure as photoinitiator mixed with human umbilical vein endothelial cells (HUVECs), VEGF conjugated GelMA, and bone marrow-derived human mesenchymal stem cells laden silicate blended GelMA solutions to print vascular core and bony peripheral regions respectively. By using these bioinks, bone-like structures analogous to the cross-sectional structure of native bone were bioprinted and stabilized using the photocrosslinking method. These printed constructs were analyzed for cytocompatibility and osteogenic ability. Remarkably, the presence of VEGF and silicate in the bioinks induced blood vessel and bone tissue formation respectively, which was confirmed by the presence of angiogenic and osteogenic markers such as Col1, CD31, OCN, OPN, ALP, and RUNX2. In addition, the printed hydrogels in core parts degraded faster within 24 h leaving an open lumen for the endothelial cells to form a softcore and printed peripheral hydrogels were stable enough for the stem cells to differentiate into osteoblasts and osteoclasts [167].

Photocrosslinking has been widely used in the extrusion-based bioprinting process, where the light energy is irradiated homogeneously either to the whole printed construct (after the printing process) or to each printed layer (layer-by-layer manner; during the printing process) [168]. Light penetration ability, pre-polymer concentration, photoinitiator concentration, exposure time, and crosslinking kinetics affect the crosslinking efficiency of the printed constructs. Further, these above factors also determine the viability and stability of the printed cell-laden constructs. For instance, printing high viscous bioink using extrusion-based bioprinting will require a longer photocrosslinking duration because shorter exposure may cause improper crosslinking due to poor penetration of light energy into the deeper regions of the printed constructs. Also, longer photo exposure may affect the viability of the extruded cells and the shape fidelity of the printed constructs. Furthermore, complete removal of unreacted polymers, photoinitiators, and reaction byproducts after the crosslinking process may also be difficult as the removal methods may harm the cells in the printed constructs. This challenge demands deeper insights into the photocrosslinking strategies for successful clinical translation.

5.5. 3D bioprinting of in vitro models and implants

With the advent of 3D bioprinting technology integrated with 3D modeling software, significant improvements have been made in the fabrication of biomimetic, vascularized *in vitro* 3D models with the desired distribution of cell types and efficacious personalized implants. In general, the flexibility and versatility of this technique have been well utilized in several pharmaceutical and medical fields such as understanding the basic mechanisms involved in the tumor microenvironment, drug development & screening applications,

allowed to form microspheres using the oil-emulsion technique and then photocrosslinked to form stable microspheres. These SKOV3/HFF cell-laden gelMA microspheres were seeded on 3D printed PCL scaffolds and placed in the sample housing unit. Further, analyses showed viable cells within the developed microspheres in the fluid channels. Interestingly, these microspheres were demonstrated to have decreased cell viability in a dose-dependent manner after exposure to various concentrations of doxorubicin for about 12 h, which was quantified based on *in situ* image analysis [179].

In addition to the *in vitro* models, 3D printed implants are also developed using photocrosslinking assisted 3D bioprinting methods for tissue engineering applications [180]. Zhai et al., developed two different bioinks made of PEGDA/laponite XLG nanoclay (bioink A) and hyaluronic acid sodium salt (HA) encapsulated primary rat osteoblasts (bioink B). Bioink A aid in promoting cell growth and gaseous transport whereas bioink B improve the uniformity, viability of the encapsulated cells, and printing efficiency. These bioinks were extruded alternatively employing a two-channel 3D bioprinting system and photo-crosslinked using UV light to form a 3D nanocomposite hydrogel construct for bone regeneration applications. Further, *in vitro* culture of the bioprinted constructs showed good cell proliferation with extended cell morphology, higher alkaline phosphatase (ALP) expression after 21 days. These results confirmed the potential of this printed construct to support osteogenic differentiation due to the release of magnesium and silicon ions. Finally, *in vivo* implantation of these scaffolds in tibial defects of 12-week-old male Sprague Dawley rats also showed excellent osteogenic potential because the conducive environment around PEG-clay was favorable for osteogenic differentiation of encapsulated osteoblasts [181].

6. Challenges and future perspectives

The basic understanding of the principles and expanding applications of photocrosslinking techniques are very vital to engineer and precisely control pre-, *in situ*- and post-crosslinking of bioinks or suitable resins for 3D bioprinting [38]. This fundamental understanding is a crucial factor to improve the applications of photocrosslinking in the development of advanced 3D tissue constructs. However, more insights into the systematic investigations of this technique are still lacking and require impactful research for the future developments of photocrosslinking methods. The use of photocrosslinking in 3D bioprinting has enabled adaptable and tailorable crosslinking methods which have strong potential in the fabrication of meaningful 3D structures with improved functionalities. As described in this review, critical considerations in this strategy lie in the careful selection of appropriate bioinks, photoinitiators, optimal light source, intensity, and exposure time.

Photocrosslinking using light-sensitive chemicals like photoinitiators raise challenges in the biocompatibility of developed constructs. Most of the photoinitiators work in the UV range and their absorption peaks are at UV wavelengths, which may affect the viability of cells. Alternatively, the wavelength of 385 nm and more will result in uniform curing of photocrosslinkable materials with high cell viability. Thus, a wavelength that is closer to visible light will make the crosslinking process easier by penetrating deep into the bioinks during bioprinting. Yet, photoinitiators that work under visible light wavelength are not explored in great detail and used for 3D bioprinting of larger tissue constructs.

Therefore, novel visible light photoinitiators can be developed and can be used for visible light-mediated photocrosslinking, which will produce constructs with less cytotoxicity when compared to UV-mediated photoinitiators [182]. Moreover, water-soluble visible light photoinitiators can be developed which could further improve the cell viability by ensuring physiological conditions during the entire process. Some photoinitiators like riboflavin-based systems have poor photoinitiation efficiency although effective in offering good cell compatibility. To overcome this, two-photon photopolymerizations is a suitable approach to produce sub-micrometer resolution structures *via* 3D printing. This two-photon photocrosslinking may not be fully biocompatible and hence future research should focus on developing two-photon initiators with good solubility and stability. Another important facet in photocrosslinking is the fundamental understanding of the light-cell interactions. To overcome the common problems in photocrosslinking like DNA damage and formation of reactive oxygen species (ROS), it is necessary to carry out detailed systematic research on the working parameters of light such as wavelength, power, and exposure time [93,183].

Stereolithography is one of the most advanced techniques for printing photosensitive hydrogel. This technique operates in a simple nozzle-free method, offers high resolution, improved cell viability, and at low cost. But many stereolithography bioprinting systems use UV as a light source which is not desirable. Therefore, this method should be made available to work under visible light for wider biomedical applications with high cell viability. Further, some of the resins used in stereolithography have UV blockers to avoid over penetration of light beyond the layer to be crosslinked. The concentration of this blocker should be adjusted to control the depth of crosslinking or a biocompatible light blocker should be used in the future to avoid the problems which may arise due to the use of UV blocker [168].

Most of the research work on 3D bioprinting has focused on using a post-crosslinking strategy, but many studies have explored the advantages of *in situ* crosslinking. *In situ* crosslinking, the desired shape is obtained instantaneously during printing and the crosslinking agent is activated to get the desired stability. *In situ* crosslinking method is desired due to its potential to create uniformly crosslinked 3D printed structures [118]. Further, near-infrared can be used as a light source to produce *in situ* hydrogels, because infrared can also penetrate deep and it is harmless. In addition to *in situ* methods, intravital crosslinking systems could be explored for different applications as there is only scanty literature on this application. Furthermore, computational modeling of these crosslinking chemistries would provide a better understanding of the impact of crosslinking on the final state of the construct this will reduce the trial and error in experiments [10]. New photocrosslinking methods, engineered bioinks, modified bioprinting methods will further strengthen the existing bioprinting methods with enhanced flexibility for fabricating different biological constructs.

3D/4D bioprinting has been emerging as a promising tool for the development of biological constructs to investigate several fundamental questions starting from cancer biology to regenerative medicine [184]. To achieve this, photopatterning of bioconstructs is one of the potential strategies where the physical, chemical and biological cues to the cells could be spatiotemporally manipulated for required applications. This methodology

could offer promising prospects in combination with the existing 3D printing methods. Considering the advantages in tuning the spatiotemporal behavior of bioprinted constructs *via* photocrosslinking, future developments will focus on improving the resolution of constructs with perfusable nature along with pre-vascularization for efficient nutrient delivery and waste exchange. Further, bioprinting of multi-material bioinks with cells remains a significant challenge to meet the demands in the fabrication of complex human-scale organs. There is a need to identify the combination of strategies with photocrosslinking in 3D bioprinting to capture the intricate features of native tissues as these technologies evolve in the future. As the understanding of photocrosslinking and bioinks rapidly expands, new methods towards clinical translation of relevant sized 3D constructs with biomimetic properties could be achieved in the future.

7. Conclusions

3D bioprinting is utilized in the fabrication of advanced cellular constructs for *in vitro* models and tissue engineering applications. Biological constructs fabricated using this method could not completely recapitulate the heterogeneity and complexity of native tissues. Most of the biomaterials investigated for use in bioprinting lack suitable properties for the fabrication of clinically relevant sized tissues and also showed a narrow range of rheological and mechanical properties making them unsuitable for successful clinical translation. To overcome this challenge, biomaterials that are photocrosslinkable are studied and explored for 3D bioprinting applications. These biomaterials are sensitive to specific light and can form crosslinked stable hydrogels upon irradiation. This approach could result in the development of constructs with intricate architecture and stability which may not be easily achieved using other crosslinking techniques. The basic understanding and application of this photocrosslinking method are very crucial for the design of a wide range of bioinks to be used in various fabrication technologies like extrusion bioprinting, and laser-assisted bioprinting. The development of biofabricated tissue needs to precisely recapitulate the chemical, geometrical and mechanical cues to achieve desired functions. Hence, it is necessary to develop a light-sensitive biomaterial with biomimetic mechanical and biological properties. Although light-based 3D bioprinting can overcome the issues related to shear stress & pressure, usage of UV or toxic light sources will lead to cytotoxic effects. Despite the availability of many crosslinking approaches, the development of more precise *in vitro* models, the development of multifunctional bioinks, controllability over the degradation of tissue constructs remains a challenge. Innovations in the photocrosslinking approach to fabricate complex and heterogeneous biological constructs with biomimetic vasculature will continuously advance in the future to overcome the above challenges.

Acknowledgments

The authors sincerely thank SASTRA Deemed University and Nano Mission (SR/NM/TP-83/2016), Department of Science & Technology (DST), Government of India for their financial support. Allen Zennifer is thankful to Innovation in Science Pursuit for Inspired Research (INSPIRE) scheme of DST, Government of India, for Junior Research Fellowship (IF150843). Prof. Kumbar acknowledges the funding support by the National Institutes of Biomedical Imaging and Bioengineering of the National Institutes of Health (#R01EB020640 and #R01EB030060); the U.S. Army Medical Research Acquisition Activity (USAMRAA), through the CDMRP Peer Reviewed Medical Research Program under Award No. W81XWH2010321.

References

- [1]. Haider A, Haider S, Rao Kummara M, Kamal T, Alghyamah AAA, Jan Iftikhar F, Bano B, Khan N, Amjid Afridi M, Soo Han S, Alrahlah A, Khan R, Advances in the scaffolds fabrication techniques using biocompatible polymers and their biomedical application: a technical and statistical review, *J. Saudi Chem. Soc.* 24 (2020) 186–215, 10.1016/j.jscs.2020.01.002.
- [2]. Eltom A, Zhong G, Muhammad A, Scaffold techniques and designs in tissue engineering functions and purposes: a review, *Adv. Mater. Sci. Eng.* 2019 (2019), 10.1155/2019/3429527.
- [3]. Jammalamadaka U, Tappa K, Recent advances in biomaterials for 3D printing and tissue, *J. Funct. Biomater.* 9 (2018), 10.3390/jfb9010022.
- [4]. Dhandapani R, Krishnan PD, Zennifer A, Kannan V, Manigandan A, Arul MR, Jaiswal D, Subramanian A, Kumbar SG, Sethuraman S, Additive manufacturing of biodegradable porous orthopaedic screw, *Bioact. Mater.* 5 (2020) 458–467, 10.1016/j.bioactmat.2020.03.009. [PubMed: 32280835]
- [5]. Deo KA, Singh KA, Peak CW, Alge DL, Gaharwar AK, Bioprinting 101: design, fabrication, and evaluation of cell-laden 3D bioprinted scaffolds, *Tissue Eng. - Part A.* 26 (2020) 318–338, 10.1089/ten.tea.2019.0298. [PubMed: 32079490]
- [6]. Merceron TK, Murphy SV, Hydrogels for 3D bioprinting applications, *Essentials 3D Biofabrication Transl*, Elsevier Inc 2015, pp. 249–270, 10.1016/B978-0-12-800972-7.00014-1.
- [7]. Benwood C, Chrenek J, Kirsch RL, Masri NZ, Richards H, Teetzen K, Willerth SM, Natural biomaterials and their use as bioinks for printing tissues, *Bioengineering* 8 (2021) 1–19, 10.3390/bioengineering8020027.
- [8]. Li X, Sun Q, Li Q, Kawazoe N, Chen G, Functional hydrogels with tunable structures and properties for tissue engineering applications, *Front. Chem.* 6 (2018) 499, 10.3389/fchem.2018.00499. [PubMed: 30406081]
- [9]. Akhtar MF, Hanif M, Ranjha NM, Methods of synthesis of hydrogels ... a review, *Saudi Pharm. J.* 24 (2016) 554–559, 10.1016/j.jsps.2015.03.022. [PubMed: 27752227]
- [10]. GhavamiNejad A, Ashammakhi N, Wu XY, Khademhosseini A, Crosslinking strategies for 3D bioprinting of polymeric hydrogels, *Small* 16 (2020) 1–30, 10.1002/smll.202002931.
- [11]. Lim KS, Galarraga JH, Cui X, Lindberg GCJ, Burdick JA, Woodfield TBF, Fundamentals and applications of photo-cross-linking in bioprinting, *Chem. Rev.* 120 (2020) 10662–10694, 10.1021/acs.chemrev.9b00812. [PubMed: 32302091]
- [12]. Zhu M, Wang Y, Ferracci G, Zheng J, Cho NJ, Lee BH, Gelatin methacryloyl and its hydrogels with an exceptional degree of controllability and batch-to-batch consistency, *Sci. Rep.* 9 (2019) 1–13, 10.1038/s41598-019-42186-x. [PubMed: 30626917]
- [13]. Cernadas T, Santos M, Miguel SP, Correia IJ, Alves P, Ferreira P, Photocurable polymeric blends for surgical application, *Materials (Basel).* 13 (2020) 1–16, 10.3390/ma13245681.
- [14]. Ozcan A, Kasikovic N, Arman Kandirmaz E, Durdevic S, Petrovic S, Highly flame retardant photocured paper coatings and printability behavior, *Polym. Adv. Technol.* 31 (2020) 2647–2658, 10.1002/pat.4991.
- [15]. Costantini M, Barbetta A, Swieszkowski W, Seliktar D, Gargioli C, Rainer A, Photocurable biopolymers for coaxial bioprinting, *Methods Mol. Biol*, Humana Press Inc 2021, pp. 45–54, 10.1007/978-1-0716-0611-7_4.
- [16]. Fonseca AC, Melchels FPW, Ferreira MJS, Moxon SR, Potjewyd G, Dargaville TR, Kimber SJ, Domingos M, Emulating human tissues and organs: a bioprinting perspective toward personalized medicine, *Chem. Rev.* 120 (2020) 11128–11174, 10.1021/acs.chemrev.0c00342. [PubMed: 32937071]
- [17]. Schwab A, Levato R, D'Este M, Piluso S, Eglin D, Malda J, Printability and shape Fidelity of bioinks in 3D bioprinting, *Chem. Rev.* 120 (2020) 11028–11055, 10.1021/acs.chemrev.0c00084. [PubMed: 32856892]
- [18]. Izadifar M, Chapman D, Babyn P, Chen X, Kelly ME, UV-assisted 3D bioprinting of nanoreinforced hybrid cardiac patch for myocardial tissue engineering, *tissue eng. - part C, Methods* 24 (2018) 74–88, 10.1089/ten.tec.2017.0346.

- [19]. Xin S, Chimene D, Garza JE, Gaharwar AK, Alge DL, Clickable PEG hydrogel microspheres as building blocks for 3D bioprinting, *Biomater. Sci.* 7 (2019) 1179–1187, 10.1039/c8bm01286e. [PubMed: 30656307]
- [20]. Xiao W, Qu X, Tan Y, Xiao J, Le Y, Li Y, Liu X, Li B, Liao X, Synthesis of photocrosslinkable hydrogels for engineering three-dimensional vascular-like constructs by surface tension-driven assembly, *Mater. Sci. Eng. C.* 116 (2020), 111143, 10.1016/j.msec.2020.111143.
- [21]. Cui X, Soliman BG, Alcalá-Orozco CR, Li J, Vis MAM, Santos M, Wise SG, Levato R, Malda J, Woodfield TBF, Rnjak-Kovacina J, Lim KS, Rapid photocrosslinking of silk hydrogels with high cell density and enhanced shape Fidelity, *Adv. Healthc. Mater.* 9 (2020) 1901667, 10.1002/adhm.201901667.
- [22]. Lim KS, Abinzano F, Bernal PN, Albillos Sanchez A, Atienza-Roca P, Otto IA, Peiffer QC, Matsusaki M, Woodfield TBF, Malda J, Levato R, One-step photoactivation of a dual-functionalized bioink as cell carrier and cartilage-binding glue for chondral regeneration, *Adv. Healthc. Mater.* 9 (2020) 1901792, 10.1002/adhm.201901792.
- [23]. Tavakoli S, Kharaziha M, Kermanpur A, Mokhtari H, Sprayable and injectable visible-light kappa-carrageenan hydrogel for in-situ soft tissue engineering, *Int. J. Biol. Macromol.* 138 (2019) 590–601, 10.1016/j.ijbiomac.2019.07.126. [PubMed: 31344417]
- [24]. Guo K, Wang H, Li S, Zhang H, Li S, Zhu H, Yang Z, Zhang L, Chang P, Zheng X, Collagen-based thiol-norbornene photoclick bio-ink with excellent bioactivity and printability, *ACS Appl. Mater. Interfaces* 13 (2021) 7037–7050, 10.1021/acsami.0c16714. [PubMed: 33517661]
- [25]. Wang Z, Jin X, Dai R, Holzman JF, Kim K, An ultrafast hydrogel photocrosslinking method for direct laser bioprinting, *RSC Adv.* 6 (2016) 21099–21104, 10.1039/c5ra24910d.
- [26]. Kumar H, Sakthivel K, Mohamed MGA, Boras E, Shin SR, Kim K, Designing gelatin methacryloyl (GelMA)-based bioinks for visible light stereolithographic 3D biofabrication, *Macromol. Biosci.* 21 (2021) 1–17, 10.1002/mabi.202000317.
- [27]. Visscher DO, Lee H, van Zuijlen PPM, Helder MN, Atala A, Yoo JJ, Lee SJ, A photo-crosslinkable cartilage-derived extracellular matrix (ECM) bioink for auricular cartilage tissue engineering, *Acta Biomater.* (2020), 10.1016/j.actbio.2020.11.029.
- [28]. Liu X, Gaihe B, George MN, Miller AL, Xu H, Waletzki BE, Lu L, 3D bioprinting of oligo(poly[ethylene glycol] fumarate) for bone and nerve tissue engineering, *J. Biomed. Mater. Res. - Part A.* 109 (2021) 6–17, 10.1002/jbm.a.37002.
- [29]. Zhang P, Wang H, Wang P, Zheng Y, Liu L, Hu J, Liu Y, Gao Q, He Y, Lightweight 3D bioprinting with point by point photocuring, *Bioact. Mater.* 6 (2021) 1402–1412, 10.1016/J.BIOACTMAT.2020.10.023. [PubMed: 33210032]
- [30]. Liu J, Miller K, Ma X, Dewan S, Lawrence N, Chung P, McCulloch AD, Chen S, Whang G, Chung P, McCulloch AD, Chen S, Direct 3D bioprinting of cardiac micro-tissues mimicking native myocardium, *Biomaterials* 256 (2020), 120204, 10.1016/j.biomaterials.2020.120204. [PubMed: 32622020]
- [31]. Tytgat L, Dobos A, Markovic M, Van Damme L, Van Hoorick J, Bray F, Thienpont H, Ottevaere H, Dubruel P, Ovsianikov A, Van Vlierberghe S, High-resolution 3D bioprinting of photo-cross-linkable recombinant collagen to serve tissue engineering applications, *Biomacromolecules* 21 (2020) 3997–4007, 10.1021/acs.biomac.0c00386. [PubMed: 32841006]
- [32]. Caliarì SR, Burdick JA, A practical guide to hydrogels for cell culture, *Nat. Methods* 13 (2016) 405–414, 10.1038/nmeth.3839. [PubMed: 27123816]
- [33]. Klimek K, Ginalska G, Proteins and peptides as important modifiers of the polymer scaffolds for tissue engineering applications—a review, *Polymers (Basel)*. 12 (2020) 844, 10.3390/POLYM12040844. [PubMed: 32268607]
- [34]. Madduma-Bandarage USK, Madihally SV, Synthetic hydrogels: synthesis, novel trends, and applications, *J. Appl. Polym. Sci.* 138 (2021) 50376, 10.1002/app.50376.
- [35]. Pereira RF, Bártolo PJ, 3D bioprinting of photocrosslinkable hydrogel constructs, *J. Appl. Polym. Sci.* 132 (2015), 10.1002/app.42458.
- [36]. Zhang W, Du A, Liu S, Lv M, Chen S, Research progress in decellularized extracellular matrix-derived hydrogels, *Regen. Ther.* 18 (2021) 88–96, 10.1016/j.reth.2021.04.002. [PubMed: 34095366]

- [37]. Jang J, Kim TG, Kim BS, Kim SW, Kwon SM, Cho DW, Tailoring mechanical properties of decellularized extracellular matrix bioink by vitamin B2-induced photo-crosslinking, *Acta Biomater.* 33 (2016) 88–95, 10.1016/j.actbio.2016.01.013. [PubMed: 26774760]
- [38]. Zheng Z, Eglin D, Alini M, Richards GR, Qin L, Lai Y, Visible light-induced 3D bioprinting technologies and corresponding bioink materials for tissue engineering: a review, *Engineering* (2020), 10.1016/j.eng.2020.05.021.
- [39]. Min KI, Yun G, Jang Y, Kim KR, Ko YH, Jang HS, Lee YS, Kim K, Kim DP, Covalent self-assembly and one-step photocrosslinking of tyrosine-rich oligopeptides to form diverse nanostructures, *Angew. Chemie - Int. Ed.* 55 (2016) 6925–6928, 10.1002/anie.201601675.
- [40]. Mu X, Sahoo JK, Cebe P, Kaplan DL, Photo-crosslinked silk fibroin for 3d printing, *Polymers (Basel)*. 12 (2020) 1–18, 10.3390/polym12122936.
- [41]. Carnes ME, Gonyea CR, Mooney RG, Njihia JW, Coburn JM, Pins GD, Horseradish peroxidase-catalyzed crosslinking of fibrin microthread scaffolds, *tissue eng. - part C, Methods* 26 (2020) 317–331, 10.1089/ten.tec.2020.0083.
- [42]. Sakai S, Ohi H, Hotta T, Kamei H, Taya M, Differentiation potential of human adipose stem cells bioprinted with hyaluronic acid/gelatin-based bioink through microextrusion and visible light-initiated crosslinking, *Biopolymers* 109 (2018) 1–8, 10.1002/bip.23080.
- [43]. Kamoun EA, Winkel A, Eisenburger M, Menzel H, Carboxylated camphorquinone as visible-light photoinitiator for biomedical application: synthesis, characterization, and application carboxylated camphorquinone as visible-light photoinitiator, *Arab. J. Chem.* 9 (2016) 745–754, 10.1016/j.arabjc.2014.03.008.
- [44]. Nikolova MP, Chavali MS, Recent advances in biomaterials for 3D scaffolds: a review, *Bioact. Mater.* 4 (2019) 271–292, 10.1016/j.bioactmat.2019.10.005. [PubMed: 31709311]
- [45]. Shen F, Li AA, Potter MA, Chang PL, Ito T, Iida-Tanaka N, Kubo K, Yoshikawa K, Koyama Y, 220. Long-term implantation of photo-crosslinked alginate microcapsules, *Mol. Ther.* 11 (2005) S87, 10.1016/j.ymthe.2005.06.223.
- [46]. Shen Y, Tang H, Huang X, Hang R, Zhang X, Wang Y, Yao X, DLP printing photocurable chitosan to build bio-constructs for tissue engineering, *Carbohydr. Polym.* 235 (2020), 115970, 10.1016/j.carbpol.2020.115970. [PubMed: 32122504]
- [47]. Chen M, Zhong M, Johnson JA, Light-controlled radical polymerization: mechanisms, methods, and applications, *Chem. Rev.* 116 (2016) 10167–10211, 10.1021/acs.chemrev.5b00671. [PubMed: 26978484]
- [48]. Eibel A, Fast DE, Gescheidt G, Choosing the ideal photoinitiator for free radical photopolymerizations: predictions based on simulations using established data, *Polym. Chem.* 9 (2018) 5107–5115, 10.1039/c8py01195h.
- [49]. Andrzejewska E, Chapter 2 - free radical photopolymerization of multifunctional monomers A2 - Baldacchini, Tommaso, Three-dimensional Microfabr. Using Two-Phot. Polym. Elsevier Inc. 2016, pp. 62–81, 10.1016/B978-0-323-35321-2/00004-2.
- [50]. Choi JR, Yong KW, Choi JY, Cowie AC, Recent advances in photo-crosslinkable hydrogels for biomedical applications, *Biotechniques* 66 (2019) 40–53, 10.2144/btn-2018-0083. [PubMed: 30730212]
- [51]. Widiyanti P, Amali MA, Aminatun, Poly(ethylene glycol)dimethacrylate - nanofibrillated cellulose bionanocomposites as injectable hydrogel for therapy of herniated nucleus pulposus patients, *J. Mater. Res. Technol.* 9 (2020) 12716–12722, 10.1016/j.jmrt.2020.08.091.
- [52]. O'Connell CD, Zhang B, Onofrillo C, Duchini S, Blanchard R, Quigley A, Bourke J, Gambhir S, Kapsa R, Di Bella C, Choong P, Wallace GG, Tailoring the mechanical properties of gelatin methacryloyl hydrogels through manipulation of the photocrosslinking conditions, *Soft Matter* 14 (2018) 2142–2151, 10.1039/c7sm02187a. [PubMed: 29488996]
- [53]. Chai Q, Jiao Y, Yu X, Hydrogels for biomedical applications: their characteristics and the mechanisms behind them, *Gels.* 3 (2017) 6, 10.3390/gels3010006. [PubMed: 30920503]
- [54]. Bertassoni LE, Cardoso JC, Manoharan V, Cristino AL, Bhise NS, Araujo WA, Zorlutuna P, Vrana NE, Ghaemmaghami AM, Dokmeci MR, Khademhosseini A, Direct-write bioprinting of cell-laden methacrylated gelatin hydrogels, *Biofabrication* 6 (2014), 10.1088/1758-5082/6/2/024105.

- [55]. Mishra V, Kumar R, Living radical polymerization: a review, *J. Sci. Res. Banaras Hindu Univ.* 56 (2012) 141–176.
- [56]. Pereira RF, Bártolo PJ, 3D photo-fabrication for tissue engineering and drug delivery, *Engineering 1* (2015) 090–112, 10.15302/J-ENG-2015015.
- [57]. Mushtaq S, Yun SJ, Jeon J, Recent advances in bioorthogonal click chemistry for efficient synthesis of radiotracers and radiopharmaceuticals, *Molecules* 24 (2019) 10.3390/molecules24193567.
- [58]. Zeng D, Zeglis BM, Lewis JS, Anderson CJ, The growing impact of bioorthogonal click chemistry on the development of radiopharmaceuticals, *J. Nucl. Med.* 54 (2013) 829–832, 10.2967/jnumed.112.115550. [PubMed: 23616581]
- [59]. Devaraj NK, The future of bioorthogonal chemistry, *ACS Cent. Sci.* 4 (2018) 952–959, 10.1021/acscentsci.8b00251. [PubMed: 30159392]
- [60]. Shih H, Lin CC, Cross-linking and degradation of step-growth hydrogels formed by thiol-ene photoclick chemistry, *Biomacromolecules* 13 (2012) 2003–2012, 10.1021/bm300752j. [PubMed: 22708824]
- [61]. Koo SPS, Stamenovi MM, Arun Prasath R, Inglis AJ, Prez FEDU, Barner-Kowollik C, Van Camp WIM, Junkers T, Limitations of radical thiol-ene reactions for polymer-polymer conjugation, *J. Polym. Sci. Part A Polym. Chem.* 48 (2010) 1699–1713, 10.1002/pola.23933.
- [62]. Pereira RF, Barrias CC, Bártolo PJ, Granja PL, Cell-instructive pectin hydrogels crosslinked via thiol-norbornene photo-click chemistry for skin tissue engineering, *Acta Biomater.* 66 (2018) 282–293, 10.1016/j.actbio.2017.11.016. [PubMed: 29128530]
- [63]. Arkenberg MR, Nguyen HD, Lin CC, Recent advances in bio-orthogonal and dynamic crosslinking of biomimetic hydrogels, *J. Mater. Chem. B* 8 (2020) 7835–7855, 10.1039/d0tb01429j. [PubMed: 32692329]
- [64]. Brown TE, Silver JS, Worrell BT, Marozas IA, Yavitt FM, Günay KA, Bowman CN, Anseth KS, Secondary photocrosslinking of click hydrogels to probe myoblast mechanotransduction in three dimensions, *J. Am. Chem. Soc.* 140 (2018) 11585–11588, 10.1021/jacs.8b07551. [PubMed: 30183266]
- [65]. Nguyen SS, Prescher JA, Developing bioorthogonal probes to span a spectrum of re-activities, *Nat. Rev. Chem.* 4 (2020) 476–489, 10.1038/s41570-020-0205-0. [PubMed: 34291176]
- [66]. Abrahamse H, Hamblin MR, New photosensitizers for photodynamic therapy, *Biochem. J.* 473 (2016) 347–364, 10.1042/BJ20150942. [PubMed: 26862179]
- [67]. Hong BM, Park SA, Park WH, Effect of photoinitiator on chain degradation of hyaluronic acid, *Biomater. Res.* 23 (2019) 19–26, 10.1186/s40824-019-0170-1. [PubMed: 31832231]
- [68]. Hölzl K, Lin S, Tytgat L, Van Vlierberghe S, Gu L, Ovsianikov A, Bioink properties before, during and after 3D bioprinting, *Biofabrication* 8 (2016), 032002, 10.1088/1758-5090/8/3/032002. [PubMed: 27658612]
- [69]. Zhou M, Lee BH, Tan LP, A dual crosslinking strategy to tailor rheological properties of gelatin methacryloyl, *Int. J. Bioprinting.* 3 (2017) 130–137, 10.18063/IJB.2017.02.003.
- [70]. Kim E, Kim MH, Song JH, Kang C, Park WH, Dual crosslinked alginate hydrogels by riboflavin as photoinitiator, *Int. J. Biol. Macromol.* 154 (2020) 989–998, 10.1016/j.ijbiomac.2020.03.134. [PubMed: 32194119]
- [71]. Shin JY, Yeo YH, Jeong JE, Park SA, Park WH, Dual-crosslinked methylcellulose hydrogels for 3D bioprinting applications, *Carbohydr. Polym.* 238 (2020), 116192, 10.1016/j.carbpol.2020.116192. [PubMed: 32299570]
- [72]. Seo JW, Shin SR, Lee MY, Cha JM, Min KH, Lee SC, Shin SY, Bae H, Injectable hydrogel derived from chitosan with tunable mechanical properties via hybrid-crosslinking system, *Carbohydr. Polym.* 251 (2021), 117036, 10.1016/j.carbpol.2020.117036. [PubMed: 33142594]
- [73]. Basara G, Yue X, Zorlutuna P, Dual crosslinked gelatin methacryloyl hydrogels for photolithography and 3D printing, *Gels.* 5 (2019), 10.3390/gels5030034.
- [74]. D G, M AM, D ED, M D, AR A, D P, 3D bioprinting of a hyaluronan bioink through enzymatic- and visible light- crosslinking, *Biofabrication* (2017) 0–30.

- [75]. Tonda-Turo C, Carmagnola I, Chiappone A, Feng Z, Ciardelli G, Hakkarainen M, Sangermano M, Photocurable chitosan as bioink for cellularized therapies towards personalized scaffold architecture, *Bioprinting*. 18 (2020), e00082, 10.1016/j.bprint.2020.e00082.
- [76]. Han WT, Jang T, Chen S, Chong LSH, Do Jung H, Song J, Improved cell viability for large-scale biofabrication with photo-crosslinkable hydrogel systems through a dual-photoinitiator approach, *Biomater. Sci.* 8 (2020) 450–461, 10.1039/c9bm01347d.
- [77]. Franco CL, Price J, West JL, Development and optimization of a dual-photoinitiator, emulsion-based technique for rapid generation of cell-laden hydrogel microspheres, *Acta Biomater.* 7 (2011) 3267–3276, 10.1016/j.actbio.2011.06.011. [PubMed: 21704198]
- [78]. Lalevée J, Blanchard N, Tehfe MA, Peter M, Morlet-Savary F, Gigmes D, Fouassier JP, Efficient dual radical/cationic photoinitiator under visible light: a new concept, *Polym. Chem.* 2 (2011) 1986–1991, 10.1039/c1py00140j.
- [79]. Soliman BG, Lindberg GCJ, Jungst T, Hooper GJ, Groll J, Woodfield TBF, Lim KS, Stepwise control of crosslinking in a one-pot system for bioprinting of low-density bioinks, *Adv. Healthc. Mater.* 9 (2020) 1–13, 10.1002/adhm.201901544.
- [80]. Mackenzie D, Ultraviolet light fights new virus, *Engineering* 6 (2020) 851–853, 10.1016/j.eng.2020.06.009. [PubMed: 32837746]
- [81]. Kulms D, Zeise E, Pöppelmann B, Schwarz T, DNA damage, death receptor activation and reactive oxygen species contribute to ultraviolet radiation-induced apoptosis in an essential and independent way, *Oncogene* 21 (2002) 5844–5851, 10.1038/sj.onc.1205743. [PubMed: 12185583]
- [82]. Lim KS, Klotz BJ, Lindberg GCJ, Melchels FPW, Hooper GJ, Malda J, Gawlitta D, Woodfield TBF, Visible light cross-linking of gelatin hydrogels offers an enhanced cell microenvironment with improved light penetration depth, *Macromol. Biosci.* 19 (2019), 10.1002/mabi.201900098.
- [83]. Goto R, Nishida E, Kobayashi S, Aino M, Ohno T, Iwamura Y, Kikuchi T, Hayashi JI, Yamamoto G, Asakura M, Mitani A, Gelatin methacryloyl–riboflavin (Gelma–rf) hydrogels for bone regeneration, *Int. J. Mol. Sci.* 22 (2021) 1–12, 10.3390/ijms22041635.
- [84]. Barbarini AL, Reyna DL, Martino DM, The effect of light intensity, film thickness, and monomer composition in styrene-based bioinspired polymers, *Green Chem. Lett. Rev.* 3 (2010) 231–237, 10.1080/17518251003730825.
- [85]. Lee C, O’Connell CD, Onofrillo C, Choong PFM, Di Bella C, Duchi S, Human articular cartilage repair: sources and detection of cytotoxicity and genotoxicity in photo-crosslinkable hydrogel bioscaffolds, *Stem Cells Transl. Med.* 9 (2020) 302–315, 10.1002/sctm.19-0192. [PubMed: 31769213]
- [86]. Ou Q, Huang K, Fu C, Huang C, Fang Y, Gu Z, Wu J, Wang Y, Nanosilver-incorporated halloysite nanotubes/gelatin methacrylate hybrid hydrogel with osteoimmunomodulatory and antibacterial activity for bone regeneration, *Chem. Eng. J.* 382 (2020), 123019, 10.1016/j.cej.2019.123019.
- [87]. Miri AK, Nieto D, Iglesias L, Goodarzi Hosseinabadi H, Maharjan S, Ruiz-Esparza GU, Khoshkhalagh P, Manbachi A, Dokmeci MR, Chen S, Shin SR, Zhang YS, Khademhosseini A, Microfluidics-enabled multimaterial maskless stereolithographic bioprinting, *Adv. Mater.* 30 (2018), e1800242, 10.1002/adma.201800242. [PubMed: 29737048]
- [88]. Wang Z, Abdulla R, Parker B, Samanipour R, Ghosh S, Kim K, A simple and high-resolution stereolithography-based 3D bioprinting system using visible light crosslinkable bioinks, *Biofabrication* 7 (2015) 45009, 10.1088/1758-5090/7/4/045009.
- [89]. Schnellbaecher A, Binder D, Bellmaine S, Zimmer A, Vitamins in cell culture media: stability and stabilization strategies, *Biotechnol. Bioeng.* 116 (2019) 1537–1555, 10.1002/bit.26942. [PubMed: 30793282]
- [90]. Noshadi I, Hong S, Sullivan KE, Shirzaei Sani E, Portillo-Lara R, Tamayol A, Shin SR, Gao AE, Stoppel WL, Black LD, Khademhosseini A, Annabi N, In vitro and in vivo analysis of visible light crosslinkable gelatin methacryloyl (GelMA) hydrogels, *Biomater. Sci.* 5 (2017) 2093–2105, 10.1039/c7bm00110j. [PubMed: 28805830]

- [91]. Wang Z, Kumar H, Tian Z, Jin X, Holzman JF, Menard F, Kim K, Visible light photoinitiation of cell-adhesive gelatin methacryloyl hydrogels for stereolithography 3D bioprinting, *ACS Appl. Mater. Interfaces* 10 (2018) 26859–26869, 10.1021/acsami.8b06607. [PubMed: 30024722]
- [92]. Sun AX, Lin H, Beck AM, Kilroy EJ, Tuan RS, Projection stereolithographic fabrication of human adipose stem cell-incorporated biodegradable scaffolds for cartilage tissue engineering, *Front. Bioeng. Biotechnol.* 3 (2015) 115, 10.3389/fbioe.2015.00115. [PubMed: 26347860]
- [93]. Nieto D, Corrales JAM, de Mora AJ, Moroni L, Fundamentals of light-cell–polymer interactions in photo-cross-linking based bioprinting, *APL Bioeng.* 4 (2020), 041502, 10.1063/5.0022693. [PubMed: 33094212]
- [94]. Dadashi-Silab S, Doran S, Yagci Y, Photoinduced electron transfer reactions for macromolecular syntheses, *Chem. Rev.* 116 (2016) 10212–10275, 10.1021/acs.chemrev.5b00586. [PubMed: 26745441]
- [95]. Yue X, Yanez CO, Yao S, Belfield KD, Selective cell death by photochemically induced pH imbalance in cancer cells, *J. Am. Chem. Soc.* 135 (2013) 2112–2115, 10.1021/ja3122312. [PubMed: 23360465]
- [96]. Kuznetsova NA, Malkov GV, Gribov BG, Photoacid generators. Application and current state of development, *Russ. Chem. Rev.* 89 (2020) 173–190, 10.1070/rcr4899.
- [97]. Mokbel H, Toufaily J, Hamieh T, Dumur F, Campolo D, Gignes D, Pierre Fouassier J, Ortyl J, Lalevée J, Specific cationic photoinitiators for near UV and visible LEDs: iodonium versus ferrocenium structures, *J. Appl. Polym. Sci.* 132 (2015) 1–10, 10.1002/app.42759. [PubMed: 25866416]
- [98]. Alonso RCB, Brandt WC, Souza-Junior EJC, Puppim-Rontani RM, Sinhoreti MAC, Photoinitiator concentration and modulated photoactivation: influence on polymerization characteristics of experimental composites, *Appl. Adhes. Sci.* 2 (2014) 1–11, 10.1186/2196-4351-2-10.
- [99]. Kang LH, Armstrong PA, Lee LJ, Duan B, Kang KH, Butcher JT, Optimizing photo-encapsulation viability of heart valve cell types in 3D printable composite hydrogels, *Ann. Biomed. Eng.* 45 (2017) 360–377, 10.1007/s10439-016-1619-1. [PubMed: 27106636]
- [100]. Xu H, Casillas J, Krishnamoorthy S, Xu C, Effects of irgacure 2959 and lithium phenyl-2,4,6-trimethylbenzoylphosphinate on cell viability, physical properties, and microstructure in 3D bioprinting of vascular-like constructs, *Biomed. Mater.* 15 (2020), 055021, 10.1088/1748-605X/ab954e. [PubMed: 32438356]
- [101]. Rostami N, Graf D, Schranzhofer L, Hild S, Hanemann T, Overcoming oxygen inhibition effect by TODA in acrylate-based ceramic-filled inks, *Prog. Org. Coatings.* 130 (2019) 221–225, 10.1016/j.porgcoat.2019.01.048.
- [102]. Belon C, Allonas X, Croutxé-Barghorn C, Lalevée J, Overcoming the oxygen inhibition in the photopolymerization of acrylates: a study of the beneficial effect of triphenylphosphine, *J. Polym. Sci. Part A Polym. Chem.* 48 (2010) 2462–2469, 10.1002/pola.24017.
- [103]. Decker C, Jenkins AD, Kinetic approach of O₂ inhibition in ultraviolet and laser-induced polymerizations, *Macromolecules* 18 (1985) 1241–1244, 10.1021/ma00148a034.
- [104]. Ligon SC, Husár B, Wutzel H, Holman R, Liska R, Strategies to reduce oxygen inhibition in photoinduced polymerization, *Chem. Rev.* 114 (2014) 577–589, 10.1021/cr3005197.
- [105]. Wang K, Ma G, Qin X, Xiao M, Nie J, Cyclic acetals as coiniciators in CQ-induced photopolymerizations, *Polym. J.* 42 (2010) 450–455, 10.1038/pj.2010.29.
- [106]. Lilly JL, Gottipati A, Cahall CF, Agoub M, Berron BJ, Comparison of eosin and fluorescein conjugates for the photoinitiation of cell-compatible polymer coatings, *PLoS One.* 13 (2018), e0190880, 10.1371/journal.pone.0190880. [PubMed: 29309430]
- [107]. Camp CP, Peterson IL, Knoff DS, Melcher LG, Maxwell CJ, Cohen AT, Wertheimer AM, Kim M, Non-cytotoxic dityrosine photocrosslinked polymeric materials with targeted elastic moduli, *Front. Chem.* 8 (2020) 173, 10.3389/fchem.2020.00173. [PubMed: 32232027]
- [108]. van Bochove B, Grijpma DW, Mechanical properties of porous photo-crosslinked poly(trimethylene carbonate) network films, *Eur. Polym. J.* 143 (2021), 110223, 10.1016/j.eurpolymj.2020.110223.

- [109]. Lantigua D, Nguyen MA, Wu X, Suvarnapathaki S, Kwon S, Gavin W, Camci-Unal G, Synthesis and characterization of photocrosslinkable albumin-based hydrogels for biomedical applications, *Soft Matter* 16 (2020) 9242–9252, 10.1039/d0sm00977f. [PubMed: 32929420]
- [110]. Shin YJ, Shafranek RT, Tsui JH, Walcott J, Nelson A, Kim DH, 3D bioprinting of mechanically tuned bioinks derived from cardiac decellularized extracellular matrix, *Acta Biomater.* 119 (2021) 75–88, 10.1016/j.actbio.2020.11.006. [PubMed: 33166713]
- [111]. Xu Y, Li D, Yin Z, He A, Lin M, Jiang G, Song X, Hu X, Liu Y, Wang J, Wang X, Duan L, Zhou G, Tissue-engineered trachea regeneration using decellularized trachea matrix treated with laser micropore technique, *Acta Biomater.* 58 (2017) 113–121, 10.1016/j.actbio.2017.05.010. [PubMed: 28546133]
- [112]. Kumar P, Ebbens S, Zhao X, Inkjet printing of mammalian cells – theory and applications, *Bioprinting* (2021), e00157, 10.1016/j.bprint.2021.e00157.
- [113]. Kim HC, Kim E, Hong BM, Park SA, Park WH, Photocrosslinked poly(γ -glutamic acid) hydrogel for 3D bioprinting, *React. Funct. Polym.* 161 (2021), 104864, 10.1016/j.reactfunctpolym.2021.104864.
- [114]. He Y, Wang F, Wang X, Zhang J, Wang D, Huang X, A photocurable hybrid chitosan/acrylamide bioink for DLP based 3D bioprinting, *Mater. Des.* 202 (2021), 109588, 10.1016/j.matdes.2021.109588.
- [115]. Li Y, Vergaelen M, Schoolaert E, Hoogenboom R, De Clerck K, Effect of crosslinking stage on photocrosslinking of benzophenone functionalized poly(2-ethyl-2-oxazoline) nanofibers obtained by aqueous electrospinning, *Eur. Polym. J.* 112 (2019) 24–30, 10.1016/j.eurpolymj.2018.12.030.
- [116]. Mora-Boza A, Włodarczyk-Biegun MK, Del Campo A, Vázquez-Lasa B, Román JS, Glycerolphosphate as an ionic crosslinker for 3D printing of multi-layered scaffolds with improved shape fidelity and biological features, *Biomater. Sci.* 8 (2020) 506–516, 10.1039/c9bm01271k.
- [117]. Ouyang L, Highley CB, Sun W, Burdick JA, A generalizable strategy for the 3D bioprinting of hydrogels from nonviscous photo-crosslinkable inks, *Adv. Mater.* 29 (2017) 1–7, 10.1002/adma.201604983.This.
- [118]. Galarraga JH, Kwon MY, Burdick JA, 3D bioprinting via an in situ crosslinking technique towards engineering cartilage tissue, *Sci. Rep.* 9 (2019) 1–12, 10.1038/s41598-019-56117-3. [PubMed: 30626917]
- [119]. O’Connell CD, Konate S, Onofrillo C, Kapsa R, Baker C, Duchi S, Eekel T, Yue Z, Beirne S, Barnsley G, Di Bella C, Choong PF, Wallace GG, Free-form co-axial bioprinting of a gelatin methacryloyl bio-ink by direct in situ photo-crosslinking during extrusion, *Bioprinting.* 19 (2020), e00087, 10.1016/j.bprint.2020.e00087.
- [120]. Urciuolo A, Poli I, Brandolino L, Raffa P, Scattolini V, Laterza C, Giobbe GG, Zambaiti E, Selmin G, Magnussen M, Brigo L, De Coppi P, Salmaso S, Giomo M, Elvassore N, Intravital three-dimensional bioprinting, *Nat. Biomed. Eng.* 4 (2020) 901–915, 10.1038/s41551-020-0568-z. [PubMed: 32572195]
- [121]. Yang K-H, Lindberg G, Soliman B, Lim K, Woodfield T, Narayan RJ, Effect of photoinitiator on precursory stability and curing depth of thiol-ene clickable gelatin, *Polymers (Basel).* 13 (2021) 1877, 10.3390/polym13111877. [PubMed: 34198796]
- [122]. Gopinathan J, Noh I, Recent trends in bioinks for 3D printing, *Biomater. Res.* 22 (2018) 1–15, 10.1186/s40824-018-0122-1. [PubMed: 29308274]
- [123]. Datta P, Barui A, Wu Y, Ozbolat V, Moncal KK, Ozbolat IT, Essential steps in bioprinting: from pre- to post-bioprinting, *Biotechnol. Adv.* 36 (2018) 1481–1504, 10.1016/j.biotechadv.2018.06.003. [PubMed: 29909085]
- [124]. Ka arevi ŽP, Rider PM, Alkildani S, Retnasingh S, Smeets R, Jung O, Ivanišević Z, Barbeck M, An introduction to 3D bioprinting: possibilities, challenges and future aspects, *Materials (Basel).* 11 (2018), 10.3390/ma11112199.
- [125]. Ligon SC, Liska R, Stampfl J, Gurr M, Mülhaupt R, Polymers for 3D printing and customized additive manufacturing, *Chem. Rev.* 117 (2017) 10212–10290, 10.1021/acs.chemrev.7b00074. [PubMed: 28756658]

- [126]. Zhou C, Ye H, Zhang F, A novel low-cost stereolithography process based on vector scanning and mask projection for high-accuracy, high-speed, high-throughput, and large-area fabrication, *J. Comput. Inf. Sci. Eng.* 15 (2015), 10.1115/1.4028848.
- [127]. Liou Frank DF, *Rapid Prototyping and Engineering Applications*, CRC Press, 2019.
- [128]. Schmidleithner C, Kalaskar DM, *Stereolithography*, Intech 2013, p. 13, 10.5772/intechopen.78147.
- [129]. Serrano-Aroca Á, Deb S, *Acrylic-based materials for biomedical and bioengineering applications*, *Acrylate Polym. Adv. Appl.*, IntechOpen, 2020, 10.5772/intechopen.91799.
- [130]. Serrano-Aroca Á, Latest improvements of acrylic-based polymer properties for biomedical applications, *Acrylic Polym. Healthc.*, InTech, 2017, 10.5772/intechopen.68996.
- [131]. Stefaniak AB, Bowers LN, Knepp AK, Luxton TP, Peloquin DM, Baumann EJ, Ham JE, Wells JR, Johnson AR, LeBouf RF, Su FC, Martin SB, Virji MA, Particle and vapor emissions from vat polymerization desktop-scale 3-dimensional printers, *J. Occup. Environ. Hyg.* 16 (2019) 519–531, 10.1080/15459624.2019.1612068. [PubMed: 31094667]
- [132]. De Gruijl FR, Van Kranen HJ, Mullenders LHF, UV-induced DNA damage, repair, mutations and oncogenic pathways in skin cancer, *J. Photochem. Photobiol. B Biol.* 63 (2001) 19–27, 10.1016/S1011-1344(01)00199-3.
- [133]. Chatterjee S, Hui PCL, wai Kan C, Thermoresponsive hydrogels and their biomedical applications: special insight into their applications in textile based transdermal therapy, *Polymers (Basel)* 10 (2018), 10.3390/polym10050480.
- [134]. Elomaa L, Keshi E, Sauer IM, Weinhart M, Development of GelMA/PCL and dECM/PCL resins for 3D printing of acellular in vitro tissue scaffolds by stereolithography, *Mater. Sci. Eng. C.* 112 (2020), 110958, 10.1016/j.msec.2020.110958.
- [135]. Schmidleithner C, Kalaskar DM, *Stereolithography, 3D Print*, InTech, 2018, 10.5772/intechopen.78147.
- [136]. Mochi F, De Matteis F, Proposito P, Burratti L, Francini R, Casalboni M, One photon 3D polymerization via direct laser writing, *Mater. Sci. Forum* 941 (2018) 2142–2147, 10.4028/www.scientific.net/MSF.941.2142.
- [137]. Yang Y, Li L, Pan Y, Sun Z, Energy consumption modeling of stereolithography-based additive manufacturing toward environmental sustainability, *J. Ind. Ecol.* 21 (2017) S168–S178, 10.1111/jiec.12589.
- [138]. Sun HB, Kawata S, Two-photon photopolymerization and 3D lithographic microfabrication, *Adv. Polym. Sci.* 170 (2004) 169–273, 10.1007/b94405.
- [139]. Delrot P, Microfabrication through a multimode optical fiber, *Opt. Express* 26 (2018) 1766–1778. [PubMed: 29402046]
- [140]. Ovsianikov A, Chichkov BN, *Two-Photon Polymerization – High Resolution 3D Laser Technology and Its Applications*, Springer, New York, NY 2008, pp. 427–446, 10.1007/978-0-387-76499-3_12.
- [141]. Farsari M, Filippidis G, Sambani K, Drakakis TS, Fotakis C, Two-photon polymerization of an eosin Y-sensitized acrylate composite, *J. Photochem. Photobiol. A Chem.* 181 (2006) 132–135, 10.1016/j.jphotochem.2005.11.025.
- [142]. Bishop ES, Mostafa S, Pakvasa M, Luu HH, Lee MJ, Wolf JM, Ameer GA, He TC, Reid RR, 3-D bioprinting technologies in tissue engineering and regenerative medicine: current and future trends, *Genes Dis.* 4 (2017) 185–195, 10.1016/j.gendis.2017.10.002. [PubMed: 29911158]
- [143]. Crook JM, *3D Bioprinting*, 1st ed. Springer US, New York, NY, 2020, 10.1007/978-1-0716-0520-2.
- [144]. Katal G, Tyagi N, Joshi A, Digital light processing and its future applications, *Int. J. Sci. Res. Publ.* 3 (2013) 2250–3153 www.ijsrp.org.
- [145]. Kim SH, Yeon YK, Lee JM, Chao JR, Lee YJ, Seo YB, Sultan MT, Lee OJ, Lee JS, Il Yoon S, Hong IS, Khang G, Lee SJ, Yoo JJ, Park CH, Precisely printable and biocompatible silk fibroin bioink for digital light processing 3D printing, *Nat. Commun.* 9 (2018) 1–14, 10.1038/s41467-018-03759-y. [PubMed: 29317637]
- [146]. Mao Q, Wang Y, Li Y, Juengpanich S, Li W, Chen M, Yin J, Fu J, Cai X, Fabrication of liver microtissue with liver decellularized extracellular matrix (dECM) bioink by digital

light processing (DLP) bioprinting, *Mater. Sci. Eng. C.* 109 (2020), 110625, 10.1016/j.msec.2020.110625.

- [147]. Hong H, Seo YB, Kim DY, Lee JS, Lee YJ, Lee H, Ajiteru O, Sultan MT, Lee OJ, Kim SH, Park CH, Digital light processing 3D printed silk fibroin hydrogel for cartilage tissue engineering, *Biomaterials* 232 (2020), 119679, 10.1016/j.biomaterials.2019.119679. [PubMed: 31865191]
- [148]. Xue D, Zhang J, Wang Y, Mei D, Digital light processing-based 3D printing of cell-seeding hydrogel scaffolds with regionally varied stiffness, *ACS Biomater. Sci. Eng.* 5 (2019) 4825–4833, 10.1021/acsbomaterials.9b00696. [PubMed: 33448825]
- [149]. Li Y, Mao Q, Li X, Yin J, Wang Y, Fu J, Huang Y, High-fidelity and high-efficiency additive manufacturing using tunable pre-curing digital light processing, *Addit. Manuf.* 30 (2019), 100889, 10.1016/j.addma.2019.100889.
- [150]. Li VCF, Kuang X, Mulyadi A, Hamel CM, Deng Y, Qi HJ, 3D printed cellulose nanocrystal composites through digital light processing, *Cellulose* 26 (2019) 3973–3985, 10.1007/s10570-019-02353-9.
- [151]. Zhu W, Qu X, Zhu J, Ma X, Patel S, Liu J, Wang P, Lai CSE, Gou M, Xu Y, Zhang K, Chen S, Direct 3D bioprinting of prevascularized tissue constructs with complex microarchitecture, *Biomaterials* 124 (2017) 106–115, 10.1016/j.biomaterials.2017.01.042. [PubMed: 28192772]
- [152]. Xu X, Tao J, Wang S, Yang L, Zhang J, Zhang J, Liu H, Cheng H, Xu J, Gou M, Wei Y, 3D printing of nerve conduits with nanoparticle-encapsulated RGFP966, *Appl. Mater. Today* 16 (2019) 247–256, 10.1016/j.apmt.2019.05.014.
- [153]. Lammel-Lindemann J, Dourado IA, Shanklin J, Rodriguez CA, Catalani LH, Dean D, Photocrosslinking-based 3D printing of unsaturated polyesters from isosorbide: a new material for resorbable medical devices, *Bioprinting.* 18 (2020), e00062, 10.1016/j.bprint.2019.e00062.
- [154]. Zhang J, Hu Q, Wang S, Tao J, Gou M, Digital light processing based three-dimensional printing for medical applications, *Int. J. Bioprinting.* 6 (2020) 12–27, 10.18063/ijb.v6i1.242.
- [155]. Wu C, Wang B, Zhang C, Wysk RA, Chen YW, Bioprinting: an assessment based on manufacturing readiness levels, *Crit. Rev. Biotechnol.* 37 (2017) 333–354, 10.3109/07388551.2016.1163321. [PubMed: 27023266]
- [156]. Cui X, Dean D, Ruggeri ZM, Boland T, Cell damage evaluation of thermal inkjet printed chinese hamster ovary cells, *Biotechnol. Bioeng.* 106 (2010) 963–969, 10.1002/BIT.22762. [PubMed: 20589673]
- [157]. Wu HC, Shan TR, Hwang WS, Lin HJ, Study of micro-droplet behavior for a piezoelectric inkjet printing device using a single pulse voltage pattern, *Mater. Trans.* 45 (2004) 1794–1801, 10.2320/MATERTRANS.45.1794.
- [158]. Wilson WC, Boland T, Cell and organ printing 1: protein and cell printers, *Anat. Rec. Part A Discov. Mol. Cell. Evol. Biol.* 272A (2003) 491–496, 10.1002/AR.A.10057.
- [159]. Xu T, Petridou S, Lee EH, Roth EA, Vyavahare NR, Hickman JJ, Boland T, Construction of high-density bacterial colony arrays and patterns by the ink-jet method, *Biotechnol. Bioeng.* 85 (2004) 29–33, 10.1002/BIT.10768. [PubMed: 14705009]
- [160]. Gao G, Schilling AF, Hubbell K, Yonezawa T, Truong D, Hong Y, Dai G, Cui X, Improved properties of bone and cartilage tissue from 3D inkjet-bioprinted human mesenchymal stem cells by simultaneous deposition and photocrosslinking in PEG-GelMA, *Biotechnol. Lett.* 37 (2015) 2349–2355, 10.1007/S10529-015-1921-2/FIGURES/4. [PubMed: 26198849]
- [161]. Cui X, Breitenkamp K, Lotz M, D’Lima D, Lima DD, Lima DD, Synergistic action of fibroblast growth factor-2 and transforming growth factor-beta1 enhances bioprinted human neocartilage formation, */pmc/articles/PMC3402696/ Biotechnol. Bioeng.* 109 (2012) 2357. (Accessed 9 November 2021).
- [162]. Derakhshanfar S, Mbeleck R, Xu K, Zhang X, Zhong W, Xing M, 3D bioprinting for biomedical devices and tissue engineering: a review of recent trends and advances, *Bioact. Mater.* 3 (2018) 144–156, 10.1016/j.bioactmat.2017.11.008. [PubMed: 29744452]
- [163]. Gu Z, Fu J, Lin H, He Y, Development of 3D bioprinting: from printing methods to biomedical applications, *Asian J. Pharm. Sci.* (2020), 10.1016/j.ajps.2019.11.003.
- [164]. Rosenblatt J, Devereux B, Wallace DG, Injectable collagen as a pH-sensitive hydrogel, *Biomaterials* 15 (1994) 985–995, 10.1016/0142-9612(94)90079-5. [PubMed: 7841296]

- [165]. Diamantides N, Wang L, Pruiksmas T, Siemiatkoski J, Dugopolski C, Shortkroff S, Kennedy S, Bonassar LJ, Correlating rheological properties and printability of collagen bioinks: the effects of riboflavin photocrosslinking and pH, *Biofabrication* 9 (2017) 10.1088/1758-5090/aa780f.
- [166]. Liu W, Zhang YS, Heinrich MA, De Ferrari F, Jang HL, Bakht SM, Alvarez MM, Yang J, Li YC, Trujillo-de Santiago G, Miri AK, Zhu K, Khoshakhlagh P, Prakash G, Cheng H, Guan X, Zhong Z, Ju J, Zhu GH, Jin X, Shin SR, Dokmeci MR, Khademhosseini A, Rapid continuous multimaterial extrusion bioprinting, *Adv. Mater.* 29 (2017), 10.1002/adma.201604630.
- [167]. Byambaa B, Annabi N, Yue K, Trujillo-de Santiago G, Alvarez MM, Jia W, Kazemzadeh-Narbat M, Shin SR, Tamayol A, Khademhosseini A, Bioprinted osteogenic and vasculogenic patterns for engineering 3D bone tissue, *Adv. Healthc. Mater.* 6 (2017), 10.1002/adhm.201700015.
- [168]. Knowlton S, Yenilmez B, Anand S, Tasoglu S, Photocrosslinking-based bioprinting: examining crosslinking schemes, *Bioprinting*. 5 (2017) 10–18, 10.1016/j.bprint.2017.03.001.
- [169]. Lust ST, Shanahan CM, Shipley RJ, Lamata P, Gentleman E, Design considerations for engineering 3D models to study vascular pathologies in vitro, *Acta Biomater.* (2021), 10.1016/j.actbio.2021.02.031.
- [170]. Ma X, Liu J, Zhu W, Tang M, Lawrence N, Yu C, Gou M, Chen S, 3D bioprinting of functional tissue models for personalized drug screening and in vitro disease modeling, *Adv. Drug Deliv. Rev.* 132 (2018) 235–251, 10.1016/j.addr.2018.06.011. [PubMed: 29935988]
- [171]. Hwang DG, Choi YM, Jang J, 3D bioprinting-based vascularized tissue models mimicking tissue-specific architecture and pathophysiology for in vitro studies, *Front. Bioeng. Biotechnol.* 9 (2021), 10.3389/fbioe.2021.685507.
- [172]. Grigoryan B, Paulsen SJ, Corbett DC, Sazer DW, Fortin CL, Zaita AJ, Greenfield PT, Calafat NJ, Gounley JP, Ta AH, Johansson F, Randles A, Rosenkrantz JE, Louis-Rosenberg JD, Galie PA, Stevens KR, Miller JS, Multivascular networks and functional intravascular topologies within biocompatible hydrogels, / pmc/articles/PMC3402696/ *Science* 364 (2019) 458–464, 10.1126/science.aav9750. [PubMed: 31048486]
- [173]. Zhang Y, Kumar P, Lv S, Xiong D, Zhao H, Cai Z, Zhao X, Recent advances in 3D bioprinting of vascularized tissues, *Mater. Des.* 199 (2021), 109398, 10.1016/J.MATDES.2020.109398.
- [174]. B Z., Organ-level vascularization: the Mars mission of bioengineering, *J. Thorac. Cardiovasc. Surg.* 159 (2020) 2003–2007, 10.1016/J.JTCVS.2019.08.128. [PubMed: 31668537]
- [175]. Charbe N, McCarron PA, Tambuwala MM, Three-dimensional bio-printing: a new frontier in oncology research, world, *J. Clin. Oncol.* 8 (2017) 21–36, 10.5306/wjco.v8.i1.21.
- [176]. Baghban R, Roshangar L, Jahanban-Esfahlan R, Seidi K, Ebrahimi-Kalan A, Jaymand M, Kolahian S, Javaheri T, Zare P, Tumor microenvironment complexity and therapeutic implications at a glance, *cell commun, Signal.* 18 (2020) 1–19, 10.1186/s12964-020-0530-4. [PubMed: 31900175]
- [177]. Datta P, Dey M, Ataie Z, Unutmaz D, Ozbolat IT, 3D bioprinting for reconstituting the cancer microenvironment, *Npj Precis. Oncol.* 4 (2020) 1–13, 10.1038/s41698-020-0121-2. [PubMed: 31934644]
- [178]. Zhu W, Castro NJ, Cui H, Zhou X, Boualam B, McGrane R, Glazer RI, Zhang LG, A 3D printed nano bone matrix for characterization of breast cancer cell and osteoblast interactions, *Nanotechnology* 27 (2016), 315103, 10.1088/0957-4484/27/31/315103. [PubMed: 27346678]
- [179]. Parrish J, Lim KS, Baer K, Hooper GJ, Woodfield TBF, A 96-well microplate bioreactor platform supporting individual dual perfusion and high-throughput assessment of simple or biofabricated 3D tissue models, *Lab Chip* 18 (2018) 2757–2775, 10.1039/c8lc00485d. [PubMed: 30117514]
- [180]. Tamay DG, Usal TD, Alagoz AS, Yucel D, Hasirci N, Hasirci V, 3D and 4D printing of polymers for tissue engineering applications, *Front. Bioeng. Biotechnol.* 7 (2019) 164, 10.3389/fbioe.2019.00164. [PubMed: 31338366]
- [181]. Zhai X, Ruan C, Ma Y, Cheng D, Wu M, Liu W, Zhao X, Pan H, Lu WW, 3D-bioprinted osteoblast-laden nanocomposite hydrogel constructs with induced micro-environments promote cell viability, differentiation, and osteogenesis both in vitro and in vivo, *Adv. Sci.* 5 (2018), 10.1002/advs.201700550.

- [182]. Smith KC, Physical and chemical changes induced in nucleic acids by ultraviolet light, *Radiat. Res.* (1966), 10.2307/3583551.
- [183]. Hoyle CE, Lee TY, Roper T, Thiol–enes: chemistry of the past with promise for the future, *J. Polym. Sci. Part A Polym. Chem.* 42 (2004) 5301–5338, 10.1002/POLA.20366.
- [184]. Ding A, Lee SJ, Ayyagari S, Tang R, Huynh CT, Alsberg E, 4D biofabrication via instantly generated graded hydrogel scaffolds, *Bioact. Mater.* (2021), 10.1016/j.bioactmat.2021.05.021.
- [185]. Zennifer Allen, Senthivelan Praseetha, Sethuraman Swaminathan, Sundaramurthi Dhakshinamoorthy, Key advances of carboxymethyl cellulose in tissue engineering & 3D bioprinting applications, *Carbohydrate Polymers* 256 (2021), 10.1016/j.carbpol.2020.117561.
- [186]. Muthu Parkkavi Sekar Harshavardhan Budharaju, Zennifer Allen, Sethuraman Swaminathan, Vermeulen Niki, Sundaramurthi Dhakshinamoorthy, Deepak M Kalaskar, Current standards and ethical landscape of engineered tissues—3D bioprinting perspective, *J. Tissue Eng.* 12 (2021), 10.1177/20417314211027677.
- [187]. Sundaramurthi Dhakshinamoorthy, Rauf Sakandar, Hauser Charlotte, 3D bioprinting technology for regenerative medicine applications, *Int. J. Bioprinting* 2 (2) (2016) 10.18063/IJB.2016.02.010.
- [188]. Rauf Sakandar, Susapto Hepi H., Kahin Kowther, Alshehri Salwa, Abdelrahman Sherin, Jordy Homing Lam Sultan Asad, Jadhav Sandip, Sundaramurthi Dhakshinamoorthy, Gao Xin, Hauser Charlotte A. E., Self-assembling tetrameric peptides allow in situ 3D bioprinting under physiological conditions, *J. Mater. Chem. B* (2021), 10.1039/D0TB02424D.

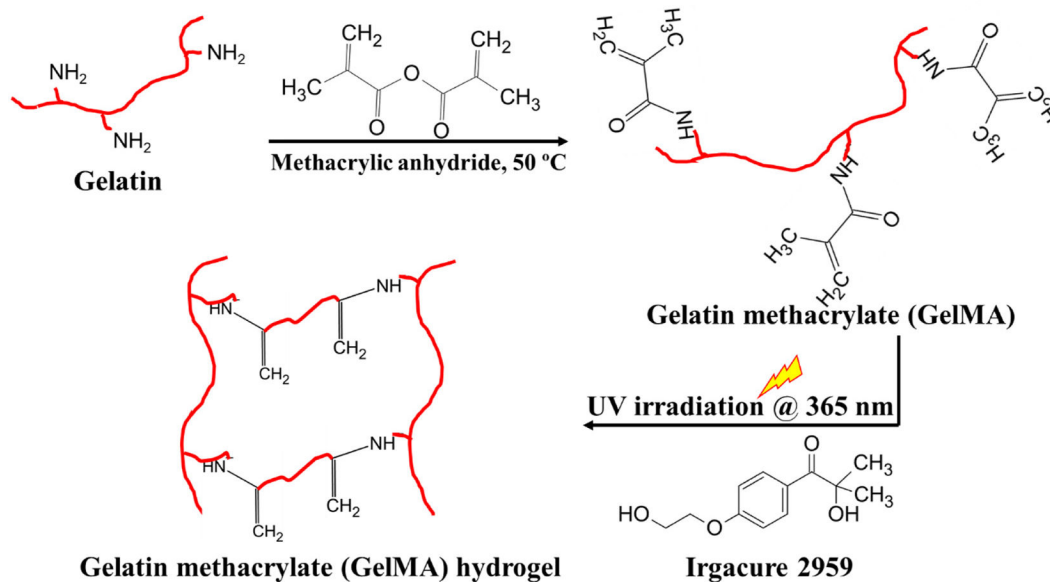


Fig. 1. General scheme of photocrosslinking of GelMA hydrogels—Gelatin methacrylate (GelMA) is obtained by modifying pristine gelatin *via* methacrylic anhydride; UV irradiation of GelMA/photoinitiator Irgacure 2959 mixture results in a stable photocrosslinked GelMA hydrogel.

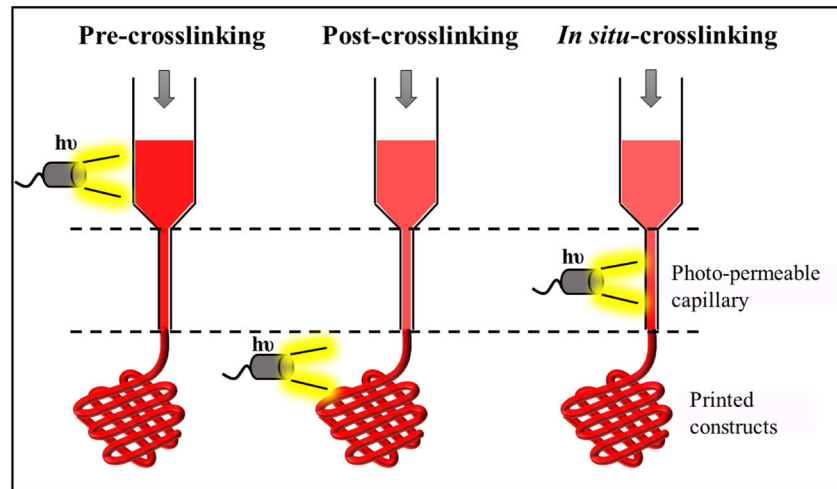


Fig. 2. Various stages involved in photocrosslinking in bioprinting technology.

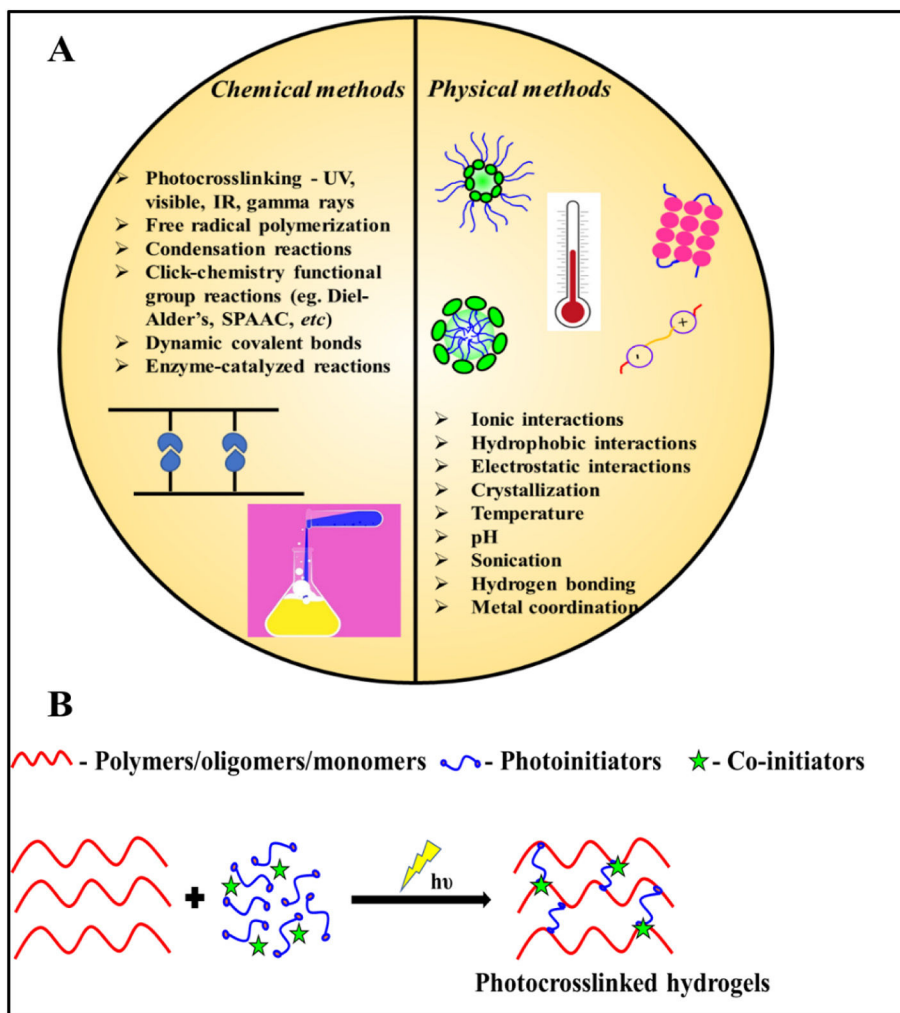


Fig. 3. (A) Various crosslinking strategies involved in hydrogel formation – Physical and chemical methods; (B) Basic components involved in the formation of photocrosslinking

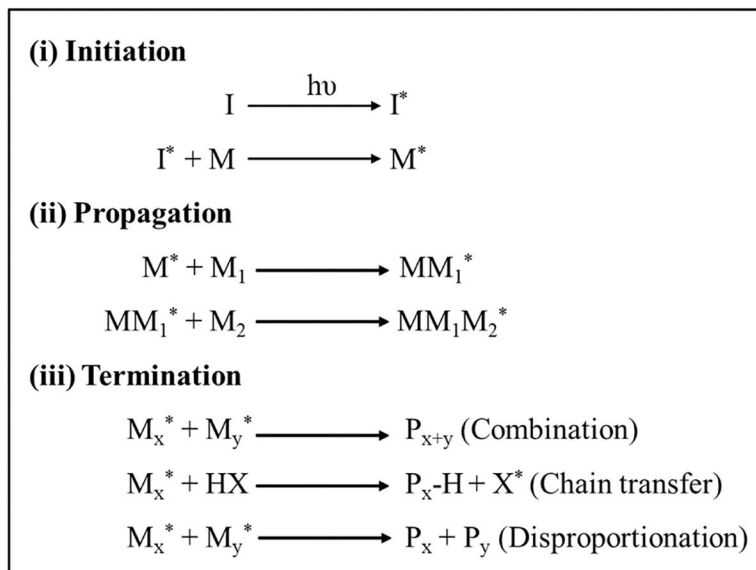


Fig. 4. Mechanism of free radical polymerization (i) Initiation: Free radicals (*) are generation *via* homolytic photolysis of photoinitiator (ii) Propagation: Rapid addition of unreacted monomers/polymers result in polymers with end-group radicals (iii) Termination: Rapid chain-growth reaction was terminated *via* radical coupling, chain transfer agents or disproportionation reactions.

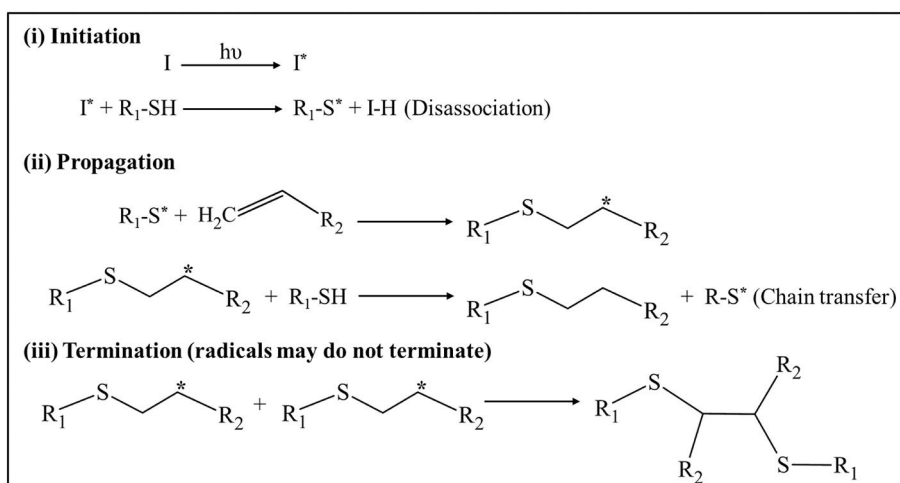


Fig. 5. Steps involved in thiol-ene polymerization reaction (i) Initiation: Generation of thiyl radicals (*) *via* irradiation of thiol functionalized photoinitiator; (ii) Propagation: Thiyl radicals react with unreacted electron-rich or strained -enes monomers/polymers yielding polymers with end-group radicals along with intermolecular thioether bonds and (iii) Termination: May terminate by disulfide bond formation *via* thiyl-thiyl radical coupling.

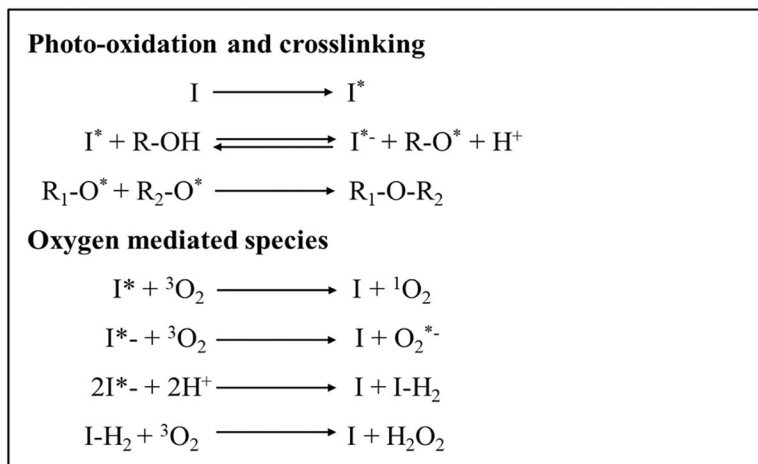


Fig. 6. Mechanism involved in redox photocrosslinking polymerization—Excited singlet state photoinitiator yield radicals forming intermolecular bonds between reactive groups. Reaction terminates only when complete consumption of photoinitiator occur.

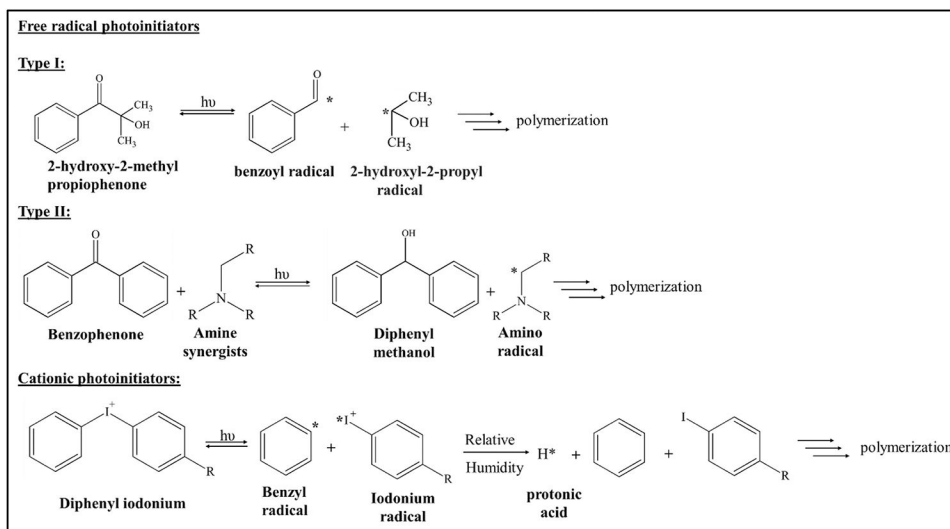


Fig. 7. Photolytic cleavage mechanism involved in photoinitiator types (i) Free radical photoinitiators—Type I: UV Irradiation of 2-hydroxy-2-methylpropiophenone yielded highly reactive benzoyl and 2-hydroxyl-2-propyl radical; Type II: Irradiation of Benzophenone by photons in the presence of amine synergists results in amine-based radicals; (ii) Cationic photoinitiators—Iodonium salt derived molecules irradiation by light energy results in iodonium radicals. The formed radicals involve in the polymerization process.

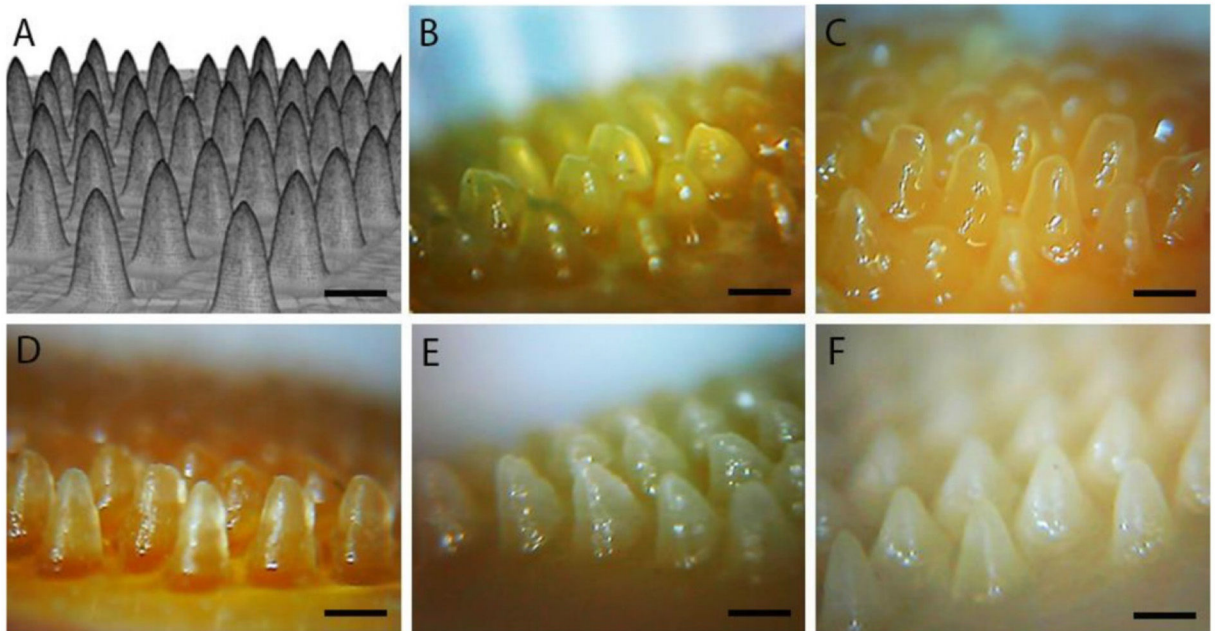


Fig. 8. (A) CAD model for fabricating human intestinal scaffold containing villi-like structures. Images (B–F) represent wet 3D printed scaffolds printed using various photocrosslinkable resins such as FGelMA (B), PGelMA (C), PCL-MA (D), FGelMA/PCL-MA, and (E) PGelMA/PCL-MA. The scale bar represents 500 μm . (Reproduced from Elomaa et al. [134]).

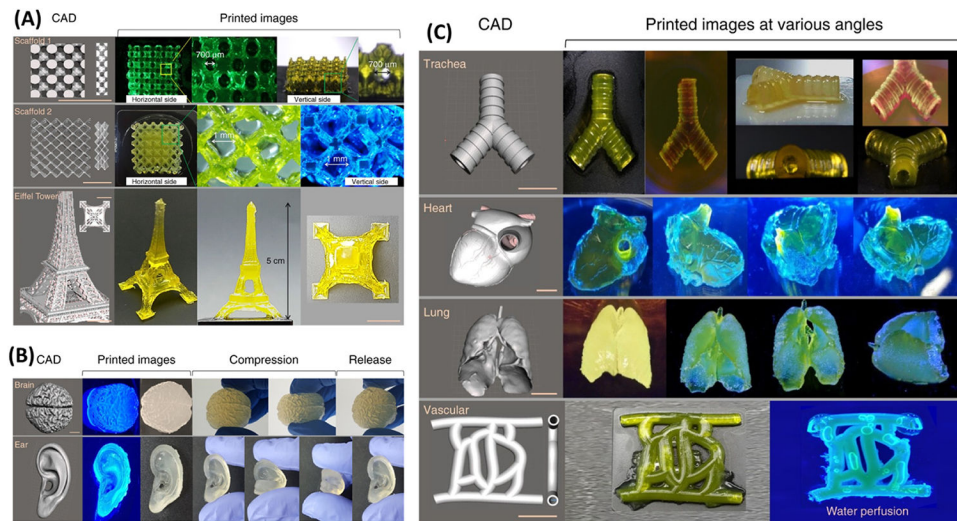


Fig. 9. Fabrication of various-shaped scaffolds printed using 30% Sil-MA *via* DLP printer (A) CAD and printed models of porous scaffold and Eiffel Tower imitation. The printed scaffolds had small pores around $\sim 700 \mu\text{m}$ and Eiffel Tower had small holes and grids on the surface (B) CAD and printed models of ear and brain mimicked structures. The printed structures were not damaged when subjected to hand compression and the structures regained its original shape. (C) CAD and printed complex-shaped models of trachea, heart, lung, and vessel mimicked constructs emphasizing the printability of Sil-MA hydrogels. Scale bar indicates 1cm. (Reproduced from Kim et al. [145]).

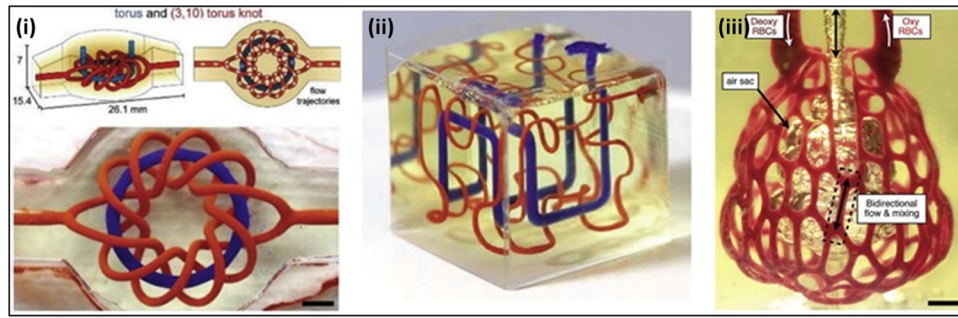


Fig. 10. Fabrication of *in vitro* 3D models: Intervascular such as Torus (i), Hilbert curve (ii) shaped patterns, and multi-vascular alveolar 3D model (iii) developed by irradiation of 20% polyethylene glycol diacrylate (PEGDA) and photoinitiator (tartrazine, curcumin, anthocyanin) solution (Reproduced from Zhang et al. [173] and Zhang et al. [174].).

Table 1

List of various functionalized polymeric biomaterials, photoinitiators, photocrosslinking parameters for 3D bioprinting of biological constructs.

Biomaterials	Photoinitiator	Photocuring parameters	Printed construct	Cell types used	Ref.
Methacrylated collagen (MeCol), Alginate coated Carbon nanotubes (CNT)	Irgacure 2959	Light source: UV Wavelength: 365 nm Irradiation time: 45 s Intensity: 6.1 mW/cm ²	3D bioprinted cardiac patch	Human coronary artery endothelial cells (HCAECs)	[18]
PEG norbornene macromers	Lithium phenyl-2,4,6-trimethylbenzoyl phosphinate (LAP)	Light source: UV Wavelength: 365 nm Irradiation time: 3 min Intensity: 60 mW/cm ²	Ear shaped construct	Human mesenchymal stem cells (hMSCs)	[19]
Methacrylated gelatin (GelMA), poly(γ -glutamic acid)	Irgacure 959	Light source: UV Irradiation time: 30 s Intensity: 8 mW/cm ²	Single-layer cylindrical construct and double-layer tubular construct	Human umbilical vascular endothelial cells (HUVECs), smooth muscle cells (HSMCs)	[20]
Silk fibroin, Gelatin	Ruthenium (Ru), Sodium per sulfate (SPS)	Light source: Visible light Wavelength: 400–450 nm Irradiation time: 3 min Intensity: 30 mW/cm ²	Grid pattern (12 × 12 mm), 7 layered constructs	Human articular chondrocytes	[21]
GelMA, tyramine	Ruthenium/sodium per sulfate	Light source: Visible light Wavelength: 450 nm	Grid pattern	Articular chondroprogenitor cells	[22]
κ -carrageenan	Eosin Y	Light source: Visible light Intensity: 100 mW/cm ² Irradiation time: 180 s	Rectangular mold (15 × 5 × 1 mm)	HeLa and fibroblasts	[23]
Norbornene-functionalized neutral soluble collagen	LAP	Light source: UV Wavelength: 365 nm Intensity: 5 mW/cm ² Irradiation time: 30 s	The pyramid side length of 9.2 mm and a height of 5 mm, monolayer tube with a diameter of 8 mm and a height of 10 mm.	Human umbilical vein endothelial cells	[24]
Gelatin methacrylate	Irgacure 2959	Light source: visible light laser Wavelength: 405 nm Intensity: 1–5 mW/mm ² Irradiation time: 10 s	Microtube pattern	NIH 3T3 fibroblast cells	[25]
Gelatin methacryloyl (GelMA)	Eosin Y, triethanol amine, <i>N</i> -vinyl caprolactam	Light source: Visible light Wavelength: 400–750 nm Intensity: 48.6 mW/cm ² Irradiation time: 60 s Irradiation distance: 10 cm	Honeycomb pattern and miniaturized multi-layered human ear and cross-section of the brain	3T3 fibroblasts, U118 astrocytes	[26]
Methacrylated auricular cartilage-derived decellularized extracellular matrix (cdECMMA), gelatin, glycerol, hyaluronic acid	Irgacure 2959	Light source: UV light Light intensity: 200 mW/cm ² Irradiation time: 2 min	Lattice and ear-shaped cell-laden constructs	Rabbit auricular chondrocytes	[27]
Oligo (poly(ethylene glycol) fumarate) (OPF),	Irgacure 2959	Light source: UV light Irradiation time: 2 min	Grid pattern with 10 mm × 10 mm width and length with 0.25 mm	MC3T3 pre-osteoblast cells and PC12 cells	[28]

Biomaterials	Photoinitiator	Photocuring parameters	Printed construct	Cell types used	Ref.
gelatin, polyethylene glycol diacrylate (PEGDA)			single layer thickness and 25% infill density		
Methacryloyl gelatin, new Coccine	LAP	Light source: visible light Wavelength: 405 nm Light source working parameters: 200 mW & 3.3 V	Grid structures with different porosities, thin-walled text structure ("EFL"), large inclined structure, thin-plate liver unit structure, and truss liver unit structures	Mouse bone marrow mesenchymal stem cells (mBMSCs)	[29]
Methacrylated gelatin, hyaluronic acid glycidyl methacrylate, polyethylene glycol diacrylate	LAP	Light source: UV light Wavelength: 365 nm Intensity: 11 mW/cm ² Irradiation time: 45 s	Slab, line, grid, dispersion, and random patterns	Neonatal mouse ventricular cardiomyocytes (NMVCMs)	[30]
Recombinant methacrylated collagen type I (RCPhCI-MA); Recombinant norbornene collagen type I (RCPhCI-NB); Recombinant thiolated collagen type I (RCPhCI-SH)	Tetrapotassium 4,4'-(1,2-ethenediyl)bis [2-(3-sulfophenyl)diazenesulfonate] (DAS)	Light source: visible light laser Wavelength: 720 nm Laser power: 10–100 mW	Cube-shaped patterns (200 × 200 × 200 μm) and different logos (TU Wien, B-PHOT, and PBM)	TERT-immortalized human adipose tissue – derived stem cell line (ASC/TERT)	[31]

Table 2

Dual crosslinking strategies for 3D bioprinting applications.

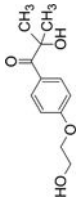
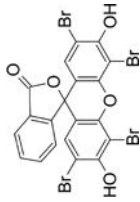
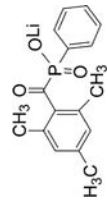
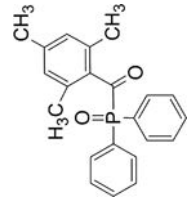
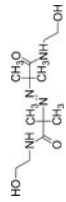
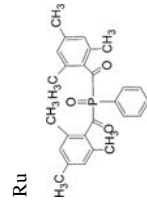
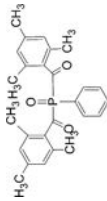
Bioink composition	Crosslinking mechanism & parameters	Significant observations	Ref
Gelatin methacryloyl (GelMA), microbial transglutaminase (mTGase), Irgacure 2959	Step 1: Enzymatic crosslinking <i>via</i> Ca ²⁺ independent mTGase Step 2: UV irradiation (365 nm, 1.5 mW/cm ²) for 5 min	<ul style="list-style-type: none"> Reduced gelation time and enhanced viscoelastic property observed for increased mTGase concentration 	[69]
Tyramine modified alginate (Alg/Tyr), Riboflavin (RF), sodium persulfate (SPS)	Homogenous ionic crosslinking by CaCO ₃ and photo-crosslinking using visible light (440 nm, 2500 mW/cm ²) for 3 min	<ul style="list-style-type: none"> Dual crosslinked hydrogels formed in a shorter gelation period had interconnected porous network, increased compressive strength of 74 kPa, and 564% swelling ratio with 36% physiological stability when compared to mono-crosslinked (photo-crosslinked) hydrogels 	[70]
Tyramine modified methylcellulose (MC-Tyr), Riboflavin (RF), Riboflavin 5'-monophosphate (RF _p), NIH3T3 fibroblasts	Step 1: Chemical crosslinking <i>via</i> conjugated carboxyl group of MC and amine groups of Tyramine; thermal crosslinking <i>via</i> methoxy groups of methyl cellulose Step 2: Visible light (440 nm, 2500 mW/cm ²) for 120 s	<ul style="list-style-type: none"> Hydrophobic and covalent interactions observed in dual crosslinked hydrogels Gelation temperature (~40 °C) of MC-Tyr remains close to physiological temperature Compressive strength and elastic modulus (4.01 kPa) of RF_p crosslinked hydrogels were higher when compared to RF crosslinked hydrogels due to the salting-out effect of the RF_p photo-initiator Bioink exhibited good printability and increased structural stability of the 3D printed scaffolds (20 × 20 × 0.2 mm) for up to 60 days in PBS Increased NIH-3T3 cell viability (~90%) was observed within the printed constructs 	[71]
Hydroxy butyl methacrylated chitosan (HBC-MA), Eosin Y, triethanolamine, 1-vinyl-2-pyrrolidone, NIH3T3 cells	Step 1: Chemical conjugation of acrylate and hydroxy butyl groups to chitosan; Thermal crosslinking at ~37 °C Step 2: Visible light (450–550 nm, 10 mW/cm ²) for 30 s	<ul style="list-style-type: none"> Hydrogels showed compact and regular porous morphology, thermo-responsiveness (20 °C), good injectability, swellability, increased storage modulus (G'), increased compressive strength, low-temperature degradability <i>In vitro</i> studies showed increased fibroblasts viability and proliferation for up to 72 h and dependent on pre-polymer concentrations Subcutaneous injection of dual crosslinked hydrogels in mice showed degradation at physiological temperature 	[72]
Gelatin methacryloyl (GelMA), microbial transglutaminase (mTGase), Irgacure 2959, human breast cancer cell line HCC1806	Step 1: Photo-crosslinking <i>via</i> acrylate groups of GelMA Step 2: Enzymatic crosslinking <i>via</i> lysine and glutamine groups of GelMA	<ul style="list-style-type: none"> Dual crosslinked hydrogels exhibited the tunable rheological and mechanical property Suitable for disease modeling applications Good printing fidelity with the visco-elastic nature of the dual crosslinked hydrogels for 3D printing applications Cytocompatible 	[73]
Tyramine modified hyaluronic acid (HA-Tyr), Eosin Y, Horse Radish Peroxidase (HRP), hydrogen peroxide (H ₂ O ₂), hTERT fibroblasts/human mesenchymal stem cells (hMSCs)/bovine chondrocytes	Step 1: Enzymatic crosslinking by HRP and H ₂ O ₂ Step 2: Visible light (505 nm) crosslinking mediated by Eosin Y	<ul style="list-style-type: none"> Cell-laden bioinks exhibited shear thinning behavior with good printability Cylindrical construct with criss-cross inner pattern (diameter—20 mm, height—1.4 mm) was printed with cells After 24 h, cell viability of extruded hMSCs, chondrocytes, and hTERT—laden bioinks was 78%, 70%, and 75% respectively Chondrocyte laden printed constructs showed higher swelling when compared to other cell-laden printed constructs 	[74]
Methacrylated chitosan, β-glycerophosphate disodium salt hydrate (β-GP), LAP, fibroblasts (NIH/3T3)/osteoblast-like cells (Saos-2)/neutrophil-like cells (SH-SY5Y)	Step 1: Thermal crosslinking <i>via</i> β-GP Step 2: UV crosslinking (365 nm, 30 mW/cm ²) for 2 min	<ul style="list-style-type: none"> Developed pCS hydrogels showed increased storage modulus and anti-oxidative property pCS cell encapsulated hydrogels showed good compatibility for up to 7 days Four layered grid-shaped constructs were printed successfully 	[75]

Table 3
Characteristic features, advantages, and disadvantages of different types of photoinitiators.

Type of photoinitiator	Free radical photoinitiator		Cationic photoinitiator	
	Type I	Type II	Type I	Type II
Mechanism of free radical generation	Unimolecular homolytic cleavage; free radicals generated	Bimolecular cleavage bond; free radicals generated	Homolytic cleavage; radicals generated as the strong acid	
Used light source & wavelengths	<ul style="list-style-type: none"> • Mostly UVA & UVB regions • LAP—365 nm • Irgacure 2959—276 nm • Irgacure 184—244, 280, 330 nm • Irgacure 651—335 nm • Diphenyl (2,4,6-trimethyl benzoyl) phosphine oxide (TPO)—272 nm 	<ul style="list-style-type: none"> • Mostly visible light regions (400–700 nm) • Eosin Y—517 nm • Riboflavin—330 to 470 nm • Camphorquinone—468 nm 	<ul style="list-style-type: none"> • Varied wavelengths—UV/visible light range • Sulfonium salts—343 nm to 372 nm • Diazonium salts—450 nm • Ferrocenium salts—617 nm 	
Advantages	<ul style="list-style-type: none"> • Very efficient in radical generation • Absorbance in short UV range • Biocompatible only when used at low concentrations • Water-soluble • Better heat and chemical resistance • Photocuring stops after removal of light • Widely used 	<ul style="list-style-type: none"> • Tissue penetration depth is higher due to long-wave UV absorbance • Better photocuring property • Biocompatible only when used at low concentrations • Water-soluble • Better heat and chemical resistance • Photocuring stops after removal of light • Widely used 	<ul style="list-style-type: none"> • Not inhibited by oxygen • Good heat and chemical resistance • Water-soluble 	
Disadvantages	<ul style="list-style-type: none"> • Yellowing of hydrogels • Bad odor • Oxygen inhibition 	<ul style="list-style-type: none"> • Require <i>co</i>-initiators to initiate photo-polymerization • Aesthetic end product due to yellowing of hydrogels—for Camphorquinone 	<ul style="list-style-type: none"> • The formation of protonic acids may cause cell damage • Curing continues even after the removal of light • Sensitivity to moisture and water 	
Applications: tissue regeneration (TE) & <i>in vitro</i> 3D Bioprinting (BP)	<p><i>In vivo</i> TE: articular cartilage [85], bone [86]</p> <p><i>In vitro</i> BP: C2C12 cells (red) and fibroblasts, breast cancer cells (MCF7), human umbilical vascular endothelial cells (HUVVECs) mesenchymal stem cells (MSCs) & osteoblasts [87], pluripotent stem cell (hiPSC)-derived hepatic progenitor cells & adipose-derived stem cells [88]</p>	<p><i>In vivo</i> TE: Cornea [89], cardiac tissues [90]</p> <p><i>In vitro</i> BP: NIH-3T3 fibroblasts [88,91], adipose stem cells [92]</p>	<p>Not suitable for biomedical applications due to protonic acid generation</p>	

Table 4

Commonly used photoinitiators and their properties.

Photoinitiator	Chemical structure	Property
Irgacure 2959		Highly effective, low odor, low volatility and can be used in waterborne photocuring system
Eosin Y		Slightly yellowish, soluble in water and sparingly soluble in alcohol, acidic dye, repeated exposure may result in blindness and systemic poisoning
LAP		Type 1 photoinitiator, water-soluble and showed increased cell viability. Showed increased absorbance at visible light wavelength
TPO		Stable, incompatible with strong oxidizing agents, possess high water solubility
VA-086		Crystalline, pale yellow, halogen-free azo-initiator
Ruthenium		The water-soluble photoinitiator changes the color of the hydrogel into yellow/red/orange
Bisacylphosphine oxide (BAPO)		Symmetric chemical structure, soluble in water but insoluble in other mono or oligomers

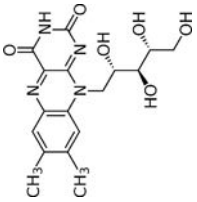
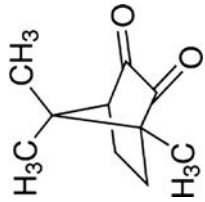
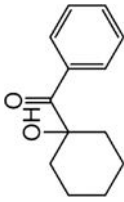
Photoinitiator	Chemical structure	Property
Riboflavin		Vitamin B2, yellow tricyclic compound, phosphorylated during the biological process
Camphorquinone		It gives a very faint fluorescence and induces polymerization very slowly
Irgacure 184		White crystalline powder with low odor and water-soluble

Table 5

3D bioprinted constructs developed using digital light processing (DLP) based 3D printing techniques.

Materials used	DLP setup	Printed tissue/cells used	Ref
Gelatin methacrylate (GelMA)/dECM	Bottom up DLP with UV (365 nm, 2.25 mW/cm ² intensity) and DMD with 1920 × 1080 resolution	Liver microtissue	[146]
Silk fibroin- Gelatin methacrylate (GelMA)	UV-LED with a wavelength of 365 nm, biconcave lenses, DMD with 30 μm resolution	Chondrocytes	[147]
Poly(ethylene glycol diacrylate) (PEGDA)	DLP system with a customized platform for printing, the light source of 405 nm wavelength, optic lenses	3T3 fibroblasts	[148]
PEGDA, Gelatin methacrylate (GelMA)	Bottom-up 3D printing system with UV of 365 nm, moving platform with 10 μm resolution in the z-axis, DMD with 1920 × 1080 resolution	PC12 cells	[149]
1,3-Diglycerolate diacrylate (DiGlyDA), PEGDA, cellulose nanocrystals (CNC)	Projector with the intensity of approximately 18 mW/cm ² is used where the resin is placed in VAT that moves in z-axis in a highly controlled manner	Acellular constructs—the disk, octet-truss lattice, and a 3D ear model	[150]
Chitosan methacrylate (CHIMA)	DLP system with blue light wavelength 405 nm, intensity 15 mW/cm ² , time 15 s and printing resolution of 800–1200 μm	Human umbilical vein endothelial cells (HUVESs)	[46]
Glycidyl methacrylate-hyaluronic acid (GM-HA)	DLP system with UV light source irradiated for 15 s	HUVESs, C3H/10T1/2 cells, HepG2 cells —vascularized tissue construct	[151]
Gelatin methacrylate (GelMA)	DLP based 3D bioprinter with 405 nm visible light wavelength and z-axis moving platform	Acellular peripheral nerve conduits seeded with Schwann cells	[152]
Hyaluronic acid glycidyl methacrylate, methacrylated gelatin	DLP (micro-continuous optical printing) system with software-controlled XYZ axis, 365 nm bandpass filter, the light intensity of 11 mW/cm ² , and irradiated for 45 s	Neonatal mouse cardiomyocytes (NMVCMs)	[30]
Isosorbide-derived polyesters	DLP device utilizes 405 nm light, 450 mW/cm ² intensity irradiated for 60 s and 150 s	Thin films seeded with fibroblasts	[153]